

An Overview of Metal Matrix Nanocomposites Reinforced with Graphene Nanoplatelets; Mechanical, Electrical and Thermophysical Properties

*Original*

An Overview of Metal Matrix Nanocomposites Reinforced with Graphene Nanoplatelets; Mechanical, Electrical and Thermophysical Properties / Saboori, Abdollah; Dadkhah, Mehran; Fino, Paolo; Pavese, Matteo. - In: METALS. - ISSN 2075-4701. - ELETTRONICO. - 8:6(2018), p. 423. [10.3390/met8060423]

*Availability:*

This version is available at: 11583/2709593 since: 2018-06-13T14:15:51Z

*Publisher:*

MDPI

*Published*

DOI:10.3390/met8060423

*Terms of use:*

This article is made available under terms and conditions as specified in the corresponding bibliographic description in the repository

*Publisher copyright*

(Article begins on next page)

Review

# An Overview of Metal Matrix Nanocomposites Reinforced with Graphene Nanoplatelets; Mechanical, Electrical and Thermophysical Properties

Abdollah Saboori \* , Mehran Dadkhah, Paolo Fino  and Matteo Pavese

Department of Applied Science and Technology, Politecnico di Torino, Corso Duca degli Abruzzi 24, 10129 Torino, Italy; mehran.dadkhah@polito.it (M.D.); Paolo.fino@polito.it (P.F.); matteo.pavese@polito.it (M.P.)

\* Correspondence: abdollah.saboori@polito.it; Tel.: +39-011-090-4762

Received: 14 May 2018; Accepted: 1 June 2018; Published: 5 June 2018



**Abstract:** Two-dimensional graphene nanoplatelets with unique electrical, mechanical and thermophysical characteristics are considered as an interesting reinforcement to develop new lightweight, high-strength, and high-performance metal matrix nanocomposites. On the other hand, by the rapid progress of technology in recent years, development of advanced materials like new metal matrix nanocomposites for structural engineering and functional device applications is a priority for various industries. This article provides an overview of research efforts with an emphasis on the fabrication and characterization of different metal matrix nanocomposites reinforced by graphene nanoplatelets (GNPs). Particular attention is devoted to find the role of GNPs on the final electrical and thermal conductivity, the coefficient of thermal expansion, and mechanical responses of aluminum, magnesium and copper matrix nanocomposites. In sum, this review pays specific attention to the structure-property relationship of these novel nanocomposites.

**Keywords:** metal matrix nanocomposite; graphene nanoplatelets; electrical conductivity; mechanical properties; thermophysical properties

---

## 1. Introduction

Metal matrix nanocomposites (MMNCs) are of great interest in recent years, mainly owing to their superior features suitable for different applications such as functional and structural applications. On the other hand, to fulfill new criteria of working conditions for electronic devices and also broaden their industrial applications in different fields such as automotive, aerospace and electronic packaging, new materials development has generated considerable research interest during the last two decades [1–9]. The technology advancement and as a result the need for devices with highly efficient are encouraged this increasing trend [10]. Nevertheless, the most accurate requirements for the choices of suitable matrix, reinforcement and techniques (processing and post-processing) are not completely defined [11]. Moreover, new facilities in the case of metal matrix nanocomposites are always suggested by the continuous progress of new materials particularly in the range of nanosize. For this reason, it is important to deeply investigate the connection between the features, constituents (including matrix), reinforcement, interphases, and also production techniques. This is one of the most interesting topics in the field of metal matrix composites. Therefore, this article aims to give its contribution by reviewing the effect of graphene nanoplatelets (GNPs) on the final properties of different MMNCs processed by additive manufacturing, casting, and powder metallurgy techniques, always keeping in mind the relationship between the materials, microstructure and final properties [12–15]. Compared to other metal matrix composites, aluminum and magnesium

matrix composites attracted a lot of interest in transportation and aeronautic applications due to their superior characteristics such as low density and high mechanical performance [4,16–18]. Furthermore, aluminum and copper composites have attracted more attention to be applied in electronic packaging and heat sink applications owing to their simultaneous high thermal and electrical conductivity and proper specific strength [19–21]. During the last years, graphene has considered as one of the most famous new nano-reinforcements [22–26]. At present, due to the specific characteristics of graphene such as high thermal and electrical conductivity, low density and very high specific strength, it is mainly investigated as a 2D reinforcement in the polymer matrix composites. However, it has not been considered as a reinforcing material in metal matrix composites until now. Therefore, this study aimed to review the effect of graphene nanoplatelets on the properties of metal matrix composites (such as electrical conductivity and mechanical performance) in particular, aluminum, magnesium and copper matrix composites.

Weight and specific strength play key roles in transportation industries such as automotive and aerospace; as such, they should be underlined as two critical parameters for the design of new composite materials [15,27–29]. Also, the reduction of fuel consumption is another new challenge that these industries are faced with and should be considered for the design of new material. Because of these facts, magnesium and aluminum alloys and their composites have attracted significant attention in research institutes and industries [30,31]. The main advantages of magnesium and aluminum are their low density, availability, and machinability features. A considerable amount of literature has been published on the fabrication and characterization of magnesium and aluminum-based composites with high specific strength so that they can be used at moderate temperatures. According to earlier research, it has proved that heat treatment or making composites can be lead to the production of an alloy with high strength [13,32]. Nevertheless, in the case of alloys which working at moderate and high temperatures such as Mg and Al-based alloys, mainly owing to the progress of artificial ageing at moderate temperature and solutioning of precipitates at high temperatures, heat treatment is not a suitable option for strengthening and thus, it seems that making of new composites is the best way for these applications. Regardless of structural applications, the presence of new materials with special characteristics such as high thermal conductivity, the tailored coefficient of thermal expansion and proper mechanical strength are the requirements in electronic packaging industries that can address the common issues in this field and increase the efficiency of devices. Copper is one of the interesting candidates applied in this field owing to its several advantages, including its very high thermal and electrical conductivity. Despite its merits, the applications of copper in electronic packaging and heatsink fields have been limited due to its shortcomings such as high coefficient of thermal expansion and moderate mechanical strength.

Powder metallurgy is considered as the main production technique of copper composites because of poor wettability between the molten copper and ceramic particles and carbon-based materials (graphene). Nevertheless, this technique involves some issues such as graphene dispersion, the best graphene content and interfacial bonding between copper and graphene, in such a way that it requires more assessments.

Previous works reported that by introducing of GNPs into a metallic matrix, some properties such as mechanical characteristics, thermal and electrical conductivities can be improved simultaneously with reduction of friction coefficients and thermal expansion. It should be mentioned that there are several main technical challenges in the fabrication of metal matrix composites, as follows: (I) reinforcement selection, (II) reinforcement dispersion, (III) reactivity between the reinforcement and matrix, (IV) interfacial bonding, and (V) preferred orientation of reinforcement. To benefit from the excellent features of the reinforcement within the metallic matrix, these technical challenges should be addressed before or within the fabrication process [33].

## 2. Materials

### 2.1. Metal Matrix Nanocomposites (MMNCs)

Composites with various chemical, physical and mechanical features can be defined as new materials including more than two constituents, with superior properties in comparison with the monolithic metal matrix [34,35]. Concerning the traditional materials, fabrication of composites would provide new conditions for modification of some characteristics such as reducing of the specific gravity, improving the mechanical properties, thermal and electrical conductivity enhancement (in some cases) [36,37]. Based on the composite matrix, these materials can be divided into three main categories including metal matrix composite (MMC), ceramic matrix composite (CMC), and polymer matrix composite (PMC) [34]. In general, it should be underlined that MMCs possess better characteristics in comparison with PMCs such as lower coefficient of thermal expansion and higher thermal and mechanical properties. Moreover, the mechanical properties of metal matrix composites such as toughness, plastic deformation and, i.e., are not comparable with CMCs [35,38,39]. The matrix of composite materials is composed of metal, ceramic or polymer material so that reinforcement is embedded inside it. In fact, light metal such as aluminum, magnesium or titanium is usually applied as a matrix in structural applications while dispersed ceramic particles or fibers are used as a reinforcement. Although, copper and copper alloys are commonly chosen as a matrix in electronic application [34].

In comparison to the matrix, a metallic matrix including reinforcement shows higher mechanical characteristics as well as physical properties like wear resistance, thermal conductivity and friction coefficient of composite [40]. It should be underlined that with focused attention to the type of reinforcement—continuous or discontinuous—different features can be achieved. In the case of metal matrix composites reinforced with a discontinuous one, owing to be isotropic materials, common metalworking techniques (such as forging, rolling or extrusion) can be applied. To fabricate an anisotropic MMC, continuous reinforcements which are mostly fibres (like carbon fibre), could be utilized [40].

Concerning the monolithic metal matrix by dispersion of reinforcement within a metallic matrix, it could be possible to fabricate a metal matrix composite with a considerable improvement in its properties. In some composites (such as Al) that reinforced by a carbonic reinforcement, to prevent any detrimental chemical reaction between the matrix and reinforcement before the composite fabrication, the reinforcement is coated [41]. Moreover, a metal matrix nanocomposite (MMNCs) can be defined as a metal matrix composite reinforced by nano-reinforcements.

As mentioned earlier, in order to the fabrication of MMNCs various metal matrices have been used, especially in the structural applications, aluminum [42–45] and magnesium [46,47] have growing trend due to their density and strength to weight properties. Whereas, in the field of electronic packaging applications, copper [48–50] matrix nanocomposites have attracted more attention. According to literature, aluminum matrix nanocomposites (AMNCs) are composed of Al or its alloys and ceramic particles or some fibers as a matrix and dispersed reinforcement, respectively. These composites have generated considerable interest due to their comparative advantages such as good mechanical properties, good processability, and low price [51]. Furthermore, the typical characteristics of AMNCs can be substantially defined as high strength, high stiffness, high thermal and electrical conductivities, and low density [35]. During the last decade, an increasing interest has been seen in the development of new lighter and high-performance of MMNCs so that it leads to rapid development of AMNCs [11,52]. Regardless of aerospace and aviation applications, this rapid development cause to extend the AMNCs application to a civil area including automotive, construction, sport and leisure application [35].

Thanks to the specific characteristics of copper matrix nanocomposites (such as their higher thermal conductivity, lower coefficient of thermal expansion and higher mechanical properties), they can support the electrical packaging applications compared to the other conductive MMNCs [53,54].

Magnesium is one of the interesting metal matrices, and is known as the lightest metal with a density of  $1.74 \text{ g/cm}^3$ . In addition, this metal is utilized as a favorable matrix to fabricate light magnesium-based nanocomposites with improved mechanical properties for using in some applications like automotive and aerospace [55,56].

As a result, it is possible to modify the characteristics of materials by made of MMNCs through the combination of a soft metal matrix with strong reinforcement and obtain MMNCs with the following features:

- Higher mechanical properties;
- Lower specific gravity;
- Improved elevated temperature properties;
- The better thermal expansion coefficient;
- Higher thermal conductivity;
- Higher wear resistance;
- Improved damping capabilities.

## 2.2. Reinforcement

Various types of reinforcements are available which present different characteristics. These reinforcements are embedded into the metal matrix nanocomposites, especially, in aluminum, copper and magnesium based composites. Based on the metallic matrix, the process of fabrication and also favourable features, the reinforcement will be chosen.

According to the composite application, the main required characteristics of a reinforcement should be considered which could be a combination of following properties; (I) comparatively low specific gravity, (II) high Young's modulus, (III) high strength, (IV) compatibility of chemical and mechanical with the matrix, (V) low coefficient of thermal expansion and (VI) economic efficiency [57].

As previously mentioned, aluminum is partly light and possesses an almost low modulus, high thermal expansion coefficient, not high strength, and medium electrical and thermal properties. Therefore, to design a new aluminum-based composite with developed properties such as higher mechanical and physical properties, the desirable low coefficient of thermal expansion, high strength, and high modulus, the choice of a proper reinforcement is essential. With the development of aluminum and copper applications in electronic packaging and so fulfills the criteria in this field, it is necessary to apply reinforcements with very high thermal conductivity and low thermal expansion coefficient. Moreover, in the reinforcements selection, it should be paid attention to their weigh (light enough), so that keeps the final composite as light as possible. In the case of magnesium alloys, their mechanical properties, particularly in high temperatures, are their main drawback. Thus it is essential to modify these disadvantages. By paying attention to these conditions, to develop new composite materials with excellent properties (such as mechanical, physical and thermal), inorganic ceramic particles or carbon-based reinforcing materials can be utilized as reinforcements [58–60].

The features of several reinforcements that can be used in metal matrix nanocomposites are compared in Table 1. As can be seen, graphene nanoplatelets (GNPs) have high strength, high hardness, and high thermal and electrical conductivity with rather low density, so it has been selected as a desirable reinforcement in recent research.

**Table 1.** The characteristics of common reinforcements [61–65].

Material	Density (g/cm <sup>3</sup> )	Thermal Conductivity (W/m·K)	Thermal Expansion Coefficient (10 <sup>6</sup> /K)	Melting Point (°C)	Vickers Hardness (HV)	Elastic Modulus (GPa)
α-Al <sub>2</sub> O <sub>3</sub>	3.95–3.98	35–39	7.1–8.4	2054–2072	1800–3000	365–393
AlN	3.05–3.26	130–180	2.5–5.3	2200–2230	1170–1530	308–346
α-SiC	3.15	42.5–270	4.3–5.8	2093–2400	2400–2500	386–476
β-SiC	3.16	135	4.5	2093 trans	2700	262–468
Diamond	3.52	2400	-	3550	8000	930
Graphite	2.25	25–470	0.6–4.3	-	-	4.8–27
SWCNTs	1.8	Up to 2900	Negligible	-	-	1000
GNPs	1.8–2.2	5300	−0.8–0.7	-	-	1000

In 2004, a single 2D layer of graphene was discovered which consisted of carbon atoms with the strong sp<sup>2</sup> band in honeycomb lattice [66]. Various allotropes of nanoscale graphitic materials are demonstrated in Figure 1 that including graphite, graphene, nanotube and fullerene.

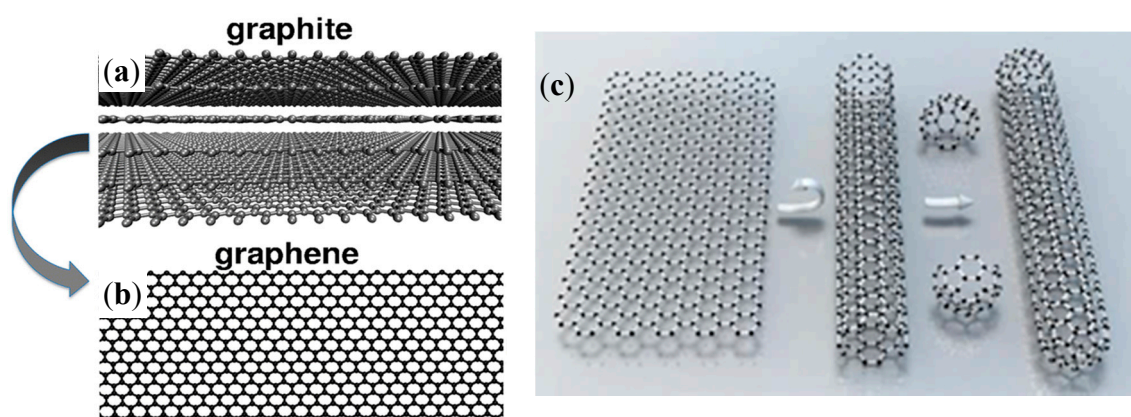


**Figure 1.** Different allotropes of carbon: (a) 3D graphite, (b) 2D graphene, (c) 1D carbon nanotubes, and 0D carbon fullerenes.

Graphene have considered as an interesting materials which could be used in several applications owing to its noticeable properties such as elastic modulus (1 TPa), the strength (130 GPa), the thermal and the electrical conductivity (5300 W/m·K and 6000 S/cm, respectively) and ultra-high surface area [67]. Furthermore, to develop new composite materials with excellent features, researchers have been persuaded to apply graphene with these fabulous characteristics as reinforcement in MMNCs.

Since 2004, a considerable amount of paper has been published on the graphene and graphene composites, as can be observed in Figure 2. For instance, in the ScienceDirect database, the number of publications on graphene has exponentially increased to several thousands of papers (more than 80,000). Consequently, the increase of graphene applications leads to the focus of researchers on its production methods. Graphene can generally be produced through two different techniques such as top-down and bottom-up. The bottom-up method is including Epitaxial growth technique [68], chemical vapor deposition (CVD) [69] and unzipping of carbon nanotubes [70] while; graphite exfoliation is considered as the top-down approach [71].

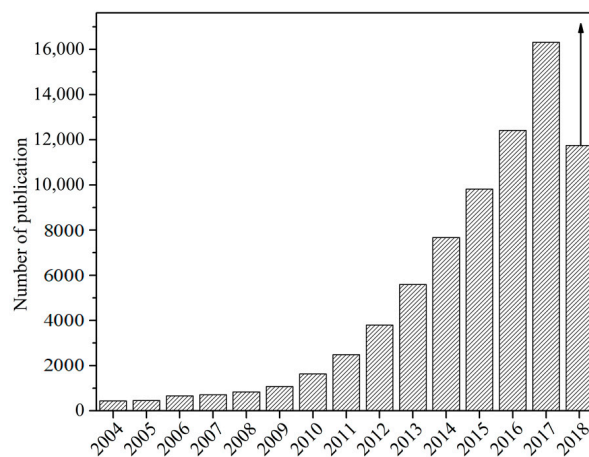


**Figure 2.** Publication trend in graphene chorology between 2004 and 2018 in ScienceDirect (this graph is plotted based on the simple searching of “graphene” at [www.sciencedirect.com](http://www.sciencedirect.com)).

As a matter of fact, graphene nanoplatelets with platelet morphology include some graphene sheets bonded to each other by interatomic Van der Waals force. In general, it is shown that the characteristics of graphene nanoplatelets in Van der Waals bonding direction are remarkably different from those displayed inside the graphitic planes [72].

As mentioned earlier, the graphene nanoplate production (such as the single layer of graphene) is divided into two techniques; top-down and bottom-up. In fact, GNPs are produced by an incomplete exfoliation process and also by bonding a single layer of graphene on the top of each other through the top-down and bottom-up techniques, respectively [71]. Moreover, GNPs are very favorable filler in MMNCs in comparison with the single layer of graphene due to their merits like higher stability, lower cost of production, easy handling and more versatility in size and aspect ratio of GNPs. It should be noted that even at the rather low graphene nanoplatelets content, a 3D network is formed and consequently anisotropic characteristics can be formed as a result of the high aspect ratio of graphene nanoplatelets within the matrix [73–77]—this improves the thermal and electrical conductivities as well as the mechanical features.

### 3. Properties of MMNCs

Metal matrix nanocomposites reinforced with nanoparticles have attracted more attention in recent years because of their promising properties concerning monolithic materials. The nano-scale particles which are used these days in the MMNCs as reinforcement have a great potential to improve the properties of the matrix. Hence, to understand the relevant mechanism of improvement and predict the effect of reinforcement on the matrix for the sake of materials design, several theoretical and experimental approaches have been proposed which are described in the following sections.

#### 3.1. Density

The ratio between total mass and total volume is known as the density of a composite material. Through the rule of mixture, it would be possible to calculate the density variations of the composite as a function of reinforcement content regardless of reinforcement distribution. Thus, the following equation can be used to calculate the density of a composite consisting of two different constituents:

$$\rho_c = \rho_p V_p + \rho_m V_m \quad (1)$$

where,  $\rho$  is the density and  $V$  is the volume fraction, and the subscripts “c”, “p” and “m” denote the composite, particle and matrix respectively. Moreover, it should be notice that the sintered density of composites can be measured according to the Archimedes method [10].

### 3.2. Thermal Properties

One of the main applications of MMNCs is in the electronic packaging industries. Thus, thermal properties such as thermal conductivity, the coefficient of thermal expansion together with mechanical properties and electrical properties, which are the main parameters in electronic package industries, have been investigated extensively.

#### 3.2.1. The Coefficient of Thermal Expansion (CTE)

Several reports have shown that to develop new composite materials for electronic packaging applications coefficient of thermal expansion of MMNCs must be investigated (in the range of  $4\sim 9 \times 10^{-6} \text{ K}^{-1}$ ). Aluminum and copper due to their unique properties such as high thermal conductivity could be good candidates for electronic packaging industries, but their high coefficient of thermal expansion limited their applications. On the other hand, graphene, which is one of the most promising 2D reinforcements with superior properties regarding thermal conductivity ( $\sim 5000 \text{ W/m}\cdot\text{K}$ ), the coefficient of thermal expansion ( $0\sim 5 \times 10^{-6} \text{ K}^{-1}$ ) and mechanical properties have been employed in the fabrication of MMNCs as a solution. These promising properties encourage the researchers to focus on using the graphene to fabricate the new composite materials with a combination of high thermal conductivity, high thermal stability and low thermal expansion coefficient. According to literature, the thermal expansion of graphene is anisotropic so that in-plane thermal expansion coefficient of graphene is  $-1 \times 10^{-6} \text{ K}^{-1}$ , while its out-of-plane CTE is  $26 \times 10^{-6} \text{ K}^{-1}$ . Thus the average CTE of polycrystalline graphene should lie in the range of  $0\sim 5 \times 10^{-6} \text{ K}^{-1}$  [78].

Based on existing literature on CTE of composite materials, there are some models available for estimating the CTE of the composites [79–81]. In fact, all the models use some assumptions and simplifications during the modeling. For instance, in the case of using the uniaxial compaction technique to fabricate the composites, it has been shown that during the compaction, graphene prefers to align perpendicular to the compaction direction (along the XY axis). This kind of preferred orientation would affect the properties of composite materials in a different axis, and thus it should be taken into account for modeling. This anisotropy in composite's characteristics was considered by a simple model proposed by Schapery [82].

$$\alpha = \frac{\alpha_a E_a V_a + \alpha_c E_c V_c + \alpha_m E_m V_m}{E_a V_a + E_c V_c + E_m V_m}, \quad (2)$$

where  $\alpha$  is the coefficient of thermal expansion,  $E$  is Young's modulus, and  $V$  is the volume fraction. The subscript "a", "c", "m" represents the in-plane and out-of-plane properties of graphene and matrix respectively.

Substantially, due to the anisotropic characteristics of graphene, the whole volume of graphene can be sorted in two parts: one part with the positive contribution of graphene in overall CTE, which is attributed to the metal/GNPs interface and another one with a negative contribution of graphene in the CTE of the composite. Therefore, it can be defined that  $V_i = c_i V_G$  ( $i = c$  and  $a$ ) and  $c_a$  and  $c_c$  are the fractions of graphene volume which plays the negative and positive roles in the final CTE. However, it should be mentioned that  $c_a + c_c = 1$  and  $V_a + V_c = V_G$ . These are the main assumption used in this modeling and by inserting these assumptions in the previous equation; the model could be as follow [78]:

$$\alpha = \frac{(\alpha_a E_a V_a + \alpha_c E_c (1 - c_a)) V_G + \alpha_m E_m V_m}{E_a V_a + E_c (1 - c_a) V_G + E_m V_m}. \quad (3)$$

In fact, by using this equation, it would be possible to predict the effect of reinforcement, in particular, graphene nanoplatelets, on the coefficient of thermal expansion of MMNCs.

### 3.2.2. Thermal Conductivity

Radiation, convection and conduction are three main mechanisms of thermal energy transportation. In general, the heat conduction feature relies seriously on the composition of a material. In fact, this feature is a transfer of the internal energy towards the lower temperature. According to the crystallographic structure and electronic characteristic of a material, the heat conduction mechanism can be changed [83]. The following formula can be used to calculate the thermal conductivity of a Material:

$$\lambda = \rho \cdot C_p \cdot \alpha, \quad (4)$$

where,  $\rho$ ,  $C_p$ ,  $\alpha$ , are density, specific heat and thermal diffusivity of material, respectively.

Substantially, heat conduction can be carried out by two mechanisms; free electrons and lattice vibration or phonons. In principle, in metals, free electrons which are present around the atomic cores can transmit both electrical current and heat through the interaction with atoms and other electrons [84]. The contribution of electrons in thermal conductivity can be calculated by the following equation [84]:

$$K_{el} = \frac{1}{3} n C_{el} v_{el} l_{el}, \quad (5)$$

where,  $n$ ,  $C_{el}$ ,  $v_{el}$ ,  $l_{el}$ , are the number of conduction electrons, electron heat capacity per electron, electron velocity and electron mean free path, respectively. Moreover, Wiedemann-Franz-Law shows the correlation between the electrical transport and thermal transport through the following equation [85]:

$$L = \frac{k_{el}}{\sigma_{el} T} = \frac{\pi^2}{3} \left( \frac{k_B}{e} \right)^2 = 2.44 \times 10^{-8} \text{ W}\Omega\text{K}^{-2}, \quad (6)$$

where,  $L$  is the Lorenz number. Since the thermal conduction in metals is carried out by electrons, they are known as best conductors like, silver (429 W/m·K), copper (385 W/m·K) and aluminum (210 W/m·K). This trend in thermal conductivity of metals, particularly in Ag, Cu, Al, is as same as their electrical conductivity. It should be noticed that the thermal conductivities of metallic materials in the literature are for pure and highly crystalline materials and these numbers can be affected by several factors such as fabrication process and impurities. For instance, it has been reported that the thermal conductivity of pure copper and copper alloys is in the range of 200–380 W/m·K [86]. Aluminum and copper are most common metallic materials which are used in electronic packaging due to their high the thermal conductivities, low cost and easy fabrication features and thus their thermal conductivity should be exploited in the case of composites.

On the other hand, it is found that due to the presence of four valence electron in the delocalized  $\pi$ -orbital of graphene, the electrical conductivity of graphene is like metals [87]. The contribution of electrons in the heat conduction of graphite through its basal plane is calculated by Wiedemann-Franz-Law, and the result shows that the electronic contribution to the heat conduction of graphite is rather low ( $K_{el} = 2.0 \text{ W/m}\cdot\text{K}$ ). Thus, it is concluded that in graphite due to its high phonon velocity and mean free path; the phonon conduction is the dominant mechanism in its thermal conductivity. This contribution (phonon conduction) can be expressed as follow:

$$K_{ph} = \frac{1}{3} C_{ph} v_{ph} l_{ph}, \quad (7)$$

where  $C_{ph}$  is the phonon heat capacity,  $v$  is the velocity of phonon,  $l$  is the mean free path of phonon [84]. Based on this equation, the thermal conductivity of graphite through the phonon conduction is estimated equal to 1910 W/m·K which is almost 1000 order of magnitude higher than its electronic conduction [88]. On the contrary, the thermal conductivity of graphite perpendicular to the basal planes is significantly lower than its basal thermal conductivity which is attributed to the strength of bonds in two different directions [89]. In fact, the strong bonding in the basal plane is covalent whereas;

the interlayer bonds are Van der Waals. However, several factors such as impurities, defects and degree of graphitization can also influence the thermal conductivity of the graphite in the basal plane.

In the case of MMNCs reinforced by high thermal conductive reinforcements such as diamond, graphene or carbon nanotubes, the mechanism of thermal conduction would be a mix of these two mechanisms, electron conduction and phonon conduction. In the literature, several theoretical models have been proposed to predict the effect of reinforcement on thermal conductivity of the MMNCs [65,90–92]. Moreover, several models have been developed to study the effect of graphene orientation on the thermal conductivity of MMNCs [90,92].

### 3.3. Mechanical Properties

Several research on MMNCs has shown that the mechanical properties of the composites, for instance, yield strength, hardness, ultimate tensile and compressive strength, can be improved through the addition of the nanoparticles [93–95]. On the contrary, it is reported that the addition of reinforcement deteriorates the ductility of MMNCs dramatically concerning the monolithic matrix [24,96]. Figure 3 shows the tensile stress-strain curves of two different aluminum based nanocomposites, and as can be seen, the reinforcement addition leads to the improvement of the tensile strength of the composite, whereas their ductility is deteriorated. This strengthening effect can be achieved through the different mechanisms including load transfer effect, Hall-Petch strengthening, thermal expansion coefficient mismatch and Orowan looping. Hence, in the previous works, the effect of different strengthening mechanisms is explained using models that can be used to forecast the yield strength [93–98].

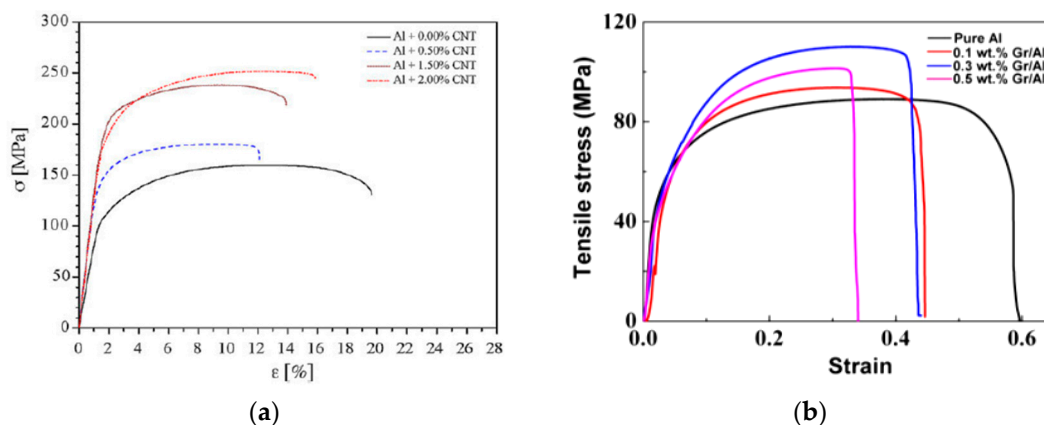


**Figure 3.** Tensile stress-strain curves of Al nanocomposites reinforced by (a) Carbon Nanotubes (CNTs)[96], (b) graphene [24], Reproduced from [96] and [24], with permission from Elsevier, 2009 and 2016.

#### 3.3.1. Load Transfer Mechanism

Load transfer effect is the first possible mechanism of strengthening in metal matrix composites. In this mechanism, load transfers from the soft matrix to high strength reinforcement and this mechanism depends on the interface between the metal and reinforcing particle. In principle, stronger interfacial bonding should result in high loading transfer and accordingly should increase the final strength of the composite. The loading transfer effect within the matrix can be explained using the following equation:

$$\Delta\sigma_{LT} = \frac{f_v \cdot \sigma_m}{2} \quad (8)$$

where  $\sigma_m$  and  $f_v$  are the yield strength of matrix and the volume fraction of reinforcement. However, it is reported that in the composites with a low reinforcement content, the load transfer effect does not contribute significantly to the strengthening of MMNCs [94,98].

### 3.3.2. Orowan Looping Mechanism

Orowan looping is another important strengthening mechanism which is based on the restriction of dislocation movement by nanoscale reinforcement. The force which is applied to each particle during its interaction with a dislocation can be calculated by [99]:

$$F = \tau b \lambda, \quad (9)$$

where,  $\tau$ ,  $\lambda$  and  $b$  are the applied stress, inter-particle spacing and the burgers vector, respectively.

In fact, whenever a particle interacts with a dislocation, it undergoes stress, and if it can withstand against the force, the dislocation starts to bow and finally an Orowan loop forms around the particle (Figure 4a). In some cases, some particles cannot withstand against the stresses applied by dislocations and they will be sheared and any dislocations loops will not form around the particles (Figure 4b). In this mechanism, uniform dispersion of reinforcement plays an important role to achieve a full strengthening effect. This strengthening effect can be expressed by the following equation:

$$\Delta\sigma_{\text{Orowan}} = \frac{0.81M \cdot G \cdot b \cdot \ln\left(\frac{d_p}{b}\right)}{2\pi\sqrt{(1-\nu)}(\lambda - d_p)}, \quad (10)$$

where,  $M$  and  $\lambda$  are the Taylor factor and the mean center to center spacing between the particles.  $G$  is the shear modulus of metal matrix,  $b$  is the burgers vector of metal matrix and  $d_p$  is the mean particle size. Here it can be notice that by decreasing the space between the graphene nanoplatelets within the matrix (through a uniform dispersion), the strengthening effect through this mechanism would increase significantly [100].

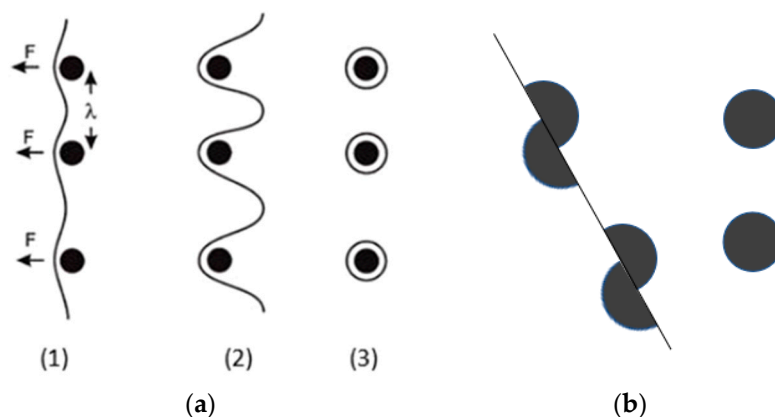


**Figure 4.** Schematic of (a) Orowan looping, (b) shearing the particles after the interaction by dislocations [100].

### 3.3.3. CTE-Mismatch Mechanism

As discussed earlier, there is a significant difference between the thermal expansion coefficient of metal matrices and reinforcing particles, in particular, graphene. This significant mismatch can result in the prismatic punching of dislocations at the interface and consequently lead to the strengthening of the composite [101]. The strengthening of composite due to the mismatch in CTE of matrix and reinforcement can be explained as follow:

$$\Delta\sigma_{\text{CTE}} = \alpha \cdot G \cdot b \sqrt{\frac{12\Delta T \cdot \Delta C \cdot f_v}{b \cdot d_p}}, \quad (11)$$

where,  $\Delta\sigma_{CTE}$  is the yield strength changes,  $\alpha$  is constant ( $\sim 1.25$ ),  $G$  is the shear modulus of metal matrix,  $b$  is the burgers vector of metal matrix,  $\Delta T$  is change in temperature,  $\Delta C$  is the difference in CTE of metal matrix and reinforcing particles,  $f_v$  is the volume fraction reinforcement and finally  $d_p$  is the mean particle size. From this equation, it is clear that due to the remarkable difference between metal matrices and reinforcing particles, a considerable strengthening effect could be predicted.

### 3.3.4. Hall-Petch Effect

Grain refinement is one of the significant effects of the reinforcement addition, and it relies on the particle size and volume fraction of nanoparticles so that the grain size ( $d_m$ ) decreases both by increasing the volume fraction of particles ( $V_p$ ) and decreasing the particle size ( $d_p$ ) [102]. This kind of relation can be explained directly through the Zener equation:

$$d_m = \frac{4\alpha d_p}{3V_p}, \quad (12)$$

where  $\alpha$  is a proportionality constant. Moreover, the Hall-Petch strengthening effect can be expressed as follow:

$$\Delta\sigma_{\text{Hall-Petch}} = \frac{k}{\sqrt{d}}, \quad (13)$$

where  $k$  and  $d$  are the Hall-Petch coefficients and average grain size of the matrix.

In the end, a theoretical model that is developed by Zhang and Chen considered all the strengthening effects in the improvement of the yield strength of the MMNCs, and it can be expressed as follow [97]:

$$\Delta\sigma = \Delta\sigma_{LT} + \Delta\sigma_{\text{Hall-Petch}} + \sqrt{(\Delta\sigma_{CTE})^2 + (\Delta\sigma_{\text{Orowan}})^2}. \quad (14)$$

## 4. Al Matrix Composites (AMCs)

Aluminum-based nanocomposites are one of the most important MMNCs commonly used in various applications such as in aerospace and automotive, but rarely in electronic packaging industries. These broad applications of Al-matrix nanocomposites are attributed to their superior features such as low density, appropriate strength, high thermals, and electrical conductivity together with low cost and easy fabrication. As mentioned earlier, several ceramic particles or allotropes of carbon are used as reinforcing materials in this kind of MMNCs. However, the most common ceramic particles used in these MMNCs are SiC, Al<sub>2</sub>O<sub>3</sub>, diamond, carbon nanotubes, graphite, and graphene. Regarding the fabrication of AMCs, two main issues have been reported in several research: one is the poor wettability of molten Al with the ceramic particles and other reinforcing materials, and another one is an undesirable reaction in the AMCs reinforced by carbonaceous reinforcement [103,104]. Several solutions have been proposed to address these issues, for instance: coating the reinforcement with an active metal to prevent the direct contact of molten Al and reinforcement [41,105,106], adding some alloying elements to increase the wettability and also prevent the reaction from the thermodynamic point of view [107–109]. Another solution is designing the process parameters in such a way that it would be possible to avoid the carbide formation reaction by using the powder metallurgy process to fabricate the AMCs [110]. As discussed earlier, the interfacial bonding is the other issue that should be considered in the fabrication of AMCs in order to take the advantages of the reinforcement [111]. Over the last decade, several efforts have been carried out to fabricate AMCs reinforced by various nano and micron ceramic particles through different fabrication techniques. For example, Al-Al<sub>2</sub>O<sub>3</sub> by SPS [112], Al-B<sub>4</sub>C by SPS and reactive infiltration [113,114], Al-MgO by stir casting and powder metallurgy [115], Al-SiC by pressureless infiltration, casting, powder metallurgy and extrusion process [116–118]. However, there is a large volume of published studies describing the role of different allotropes of carbon on mechanical properties of the AMCs and some of these efforts are listed in the following 611e (Table 2). As can be seen, these extensive efforts on AMCs reinforced by carbon-based materials

are concentrated on the strengthening effect of different reinforcements which is vital in their structural applications. Nevertheless, so far, very little attention has been paid to the role of superconductive reinforcements such as graphene on thermal behaviour of AMCs.

Pérez-Bustamante [5] and coworkers have fabricated the Al/GNPs nanocomposites by mechanical alloying followed by conventional press-sintering, and they found that the hardness of the composite increases by increasing the graphene content. Bartolucci et al. [119] studied the effect of graphene on mechanical properties of pure aluminum. They produced the Al/GNPs nanocomposite by ball-milling followed by hot isostatic pressing (HIP) and hot extrusion. According to their report, due to the formation of aluminum carbide the mechanical properties of the composites were worse than monolithic aluminum. Li et al. [120] prepared Al/graphene composite through the combination of cryomilling and hot extrusion and they found that the graphene content plays an important role in the final strength of AMCs so that by increasing the graphene content to more than 1.0 wt % due to the formation of graphene clusters the strength of composite was deteriorated. Zhang et al. [16], fabricated Al5083/GNPs composites by the combination of ball-milling and hot extrusion processes and they also found aluminum carbide in their final composite. Nonetheless, they have reported that the tensile strength of composites was improved significantly (up to 50%) by increasing the graphene content. Recently, Gao et al. [24], studied the effect of graphene nanoplatelets on mechanical properties of pure Al and they found that by increasing the graphene content the fracture mechanism of the composite changes from ductile fracture to brittle fracture. Hu et al. [121] have studied the characteristics of Al/GNPs nanocomposites produced by 3D printing. In this work, the mixture of Al/GNPs powders was prepared by ball-milling with various graphene contents then sintered by the selective laser melting (SLM) to produce bulk Gr-Al composites. Their experimental results confirmed the presence of GNPs in the composites with no physical change in its structure. Nonetheless, Raman analysis showed that the defects of graphene sheets increased. Their X-ray diffraction (XRD) patterns confirmed the formation  $Al_4C_3$  in the composites. TEM and HRTEM images further proved that graphene existed in the fabricated composites (Figure 5). Figure 6a,b shows the mechanical properties of Al and Al/GNPs nanocomposites produced by SLM. As it can be seen, by increasing the GNPs content the Vickers hardness of composites increases by nearly 75.3% compared to the laser 3D printing pure Al. The nanoindentation tests show a similar trend. These results proved that GNPs is a promising reinforcement for Al matrix and laser-based 3D printing technology can be employed to produce bulk Al/GNPs composites.

**Table 2.** A summary of recent research on AMCs reinforced by carbon allotropes.

Matrix	Reinforcement <sup>a</sup>	Content (wt %)	Fabrication Technique <sup>b</sup>	Mechanical Properties <sup>c</sup>	Ref.
Al	CNOs	1.2	HC + HEX	TS: 384 MPa	[122]
Al	CNTs	2.1	CVD	CS: 380 MPa	[123]
Al	CNTs	0.5–1.0	HR	TS: 90–200 MPa HV: 44–56	[105]
Al	Cu coated CNTs	0.5–1.0	HR	TS: 90–160 MPa HV: 61–79	[105]
Al	FLG	0.7 vol %	BM + HR	TS: 440 MPa	[124]
Al-Cu-Mg	GNFs	0.15–0.5	HIP + EX	TS: 370–460 MPa E: 72 MPa	[125]
Al	GNFs	0.5–1.0	Cryomilling + HEX	TS: 173–248 MPa	[120]
Al	GNPs	0.1	BM + HIP + EX	TS: 260 MPa HV: 84	[119]
Al	GNPs	0.25–1.0	BM + CPM	CS: 180 MPa HV: 70	[5]
Al	GNPs	0.25–1.0	HC+ HEX	TS: 166–203 MPa HV: 80–90	[126]
Al5083	GNPs	0.5–1.0	BM + HEX	TS: 434–470 MPa	[16]
Al	GNS	0.3	CPM + EX	TS: 249 MPa	[3]
Al	Graphene	0.1–0.5	HP	TS: 95–110 MPa	[24]
Al7055	Graphene	1.0–5.0	SPS	CS: 600–1200 MPa HV: 90–150	[25]
Al	Graphene sheets	2	Liquid state	TS: 48.1 MPa HV: 57.19 E: 87.93 MPa	[20]
Al	Graphite	2	Liquid state	TS: 43.92 MPa HV: 25.52 E: 58.54 MPa	[20]
Al	RGO	0.25–1.0	BM + CPM	HV: 31.63	[127]
Al-6061	SCFs	10	Pressure infiltration	TS: 127.7 MPa	[41]
Al-6061	GNPs	1	BM + HC	FS: 800 MPa	[128]

<sup>a</sup> SCFs: Short Carbon Fibers, CNOs: Carbon Nano-Onions, CNTs: Carbon Nanotubes; CFs: Carbon Fibers, FLG: Few-Layer Graphene, GNFs: Graphene Nanoflakes, GNPs: Graphene Nanoplatelets, RGO: Reduced Graphene; <sup>b</sup> CPM: Conventional Powder Metallurgy, HC: Hot Compaction, HR: Hot Rolling, HEX: Hot Extrusion, EX: Extrusion, BM: Ball-Milling, HIP: Hot Isostatic press, HP: Hot Press, SPS: Spark Plasma Sintering; <sup>c</sup> ST: Tensile strength, CS: Compressive strength, E: Elastic modulus, FS: Flexural Strength.

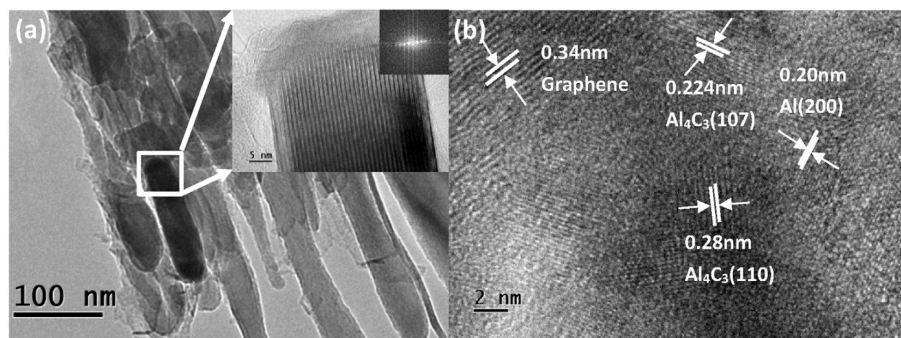


**Figure 5.** Transmission electron microscopy (TEM) and high-resolution transmission electron microscopy (HRTEM) images of Al/GNPs composites: (a) TEM image shows rod aluminum carbide with corresponding selected area diffraction (SAED) patterns, (b) graphene, Al, aluminum carbide area and their interface [121], Reproduced from [121], with permission from Elsevier, 2018.

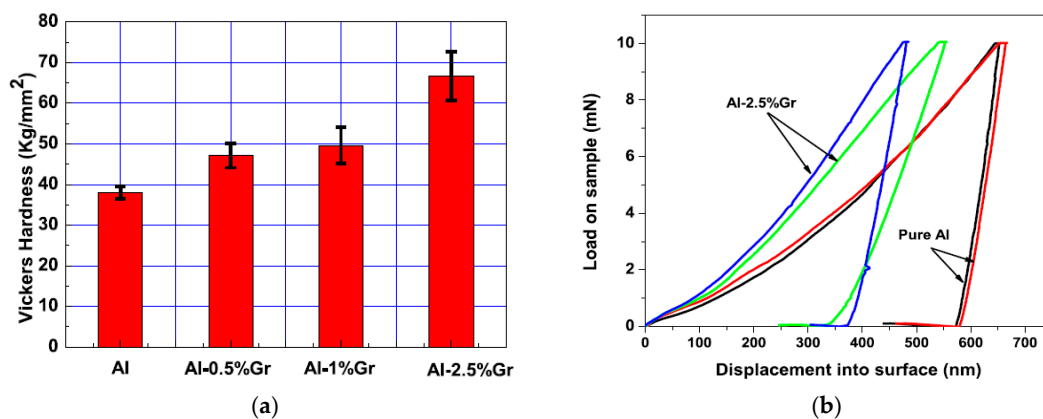


**Figure 6.** (a) The Vickers hardness and (b) load-displacement depth of nanomechanical tests of Al/GNPs nanocomposites produced by SLM [121], Reproduced from [121], with permission from Elsevier, 2018.

In another work, Saboori et al. have studied the effect of GNPs on the compressibility and sinterability of Al/GNPs nanocomposites [129]. It is found that the mechanism of consolidation for Al/GNPs at lower compaction pressures (<500 MPa) is particle rearrangement and at higher compaction pressures (>500 MPa) is plastic deformation of particles. Moreover, it is revealed that by increasing the graphene content both the compressibility and sinterability of composites decreases significantly (Figure 7).

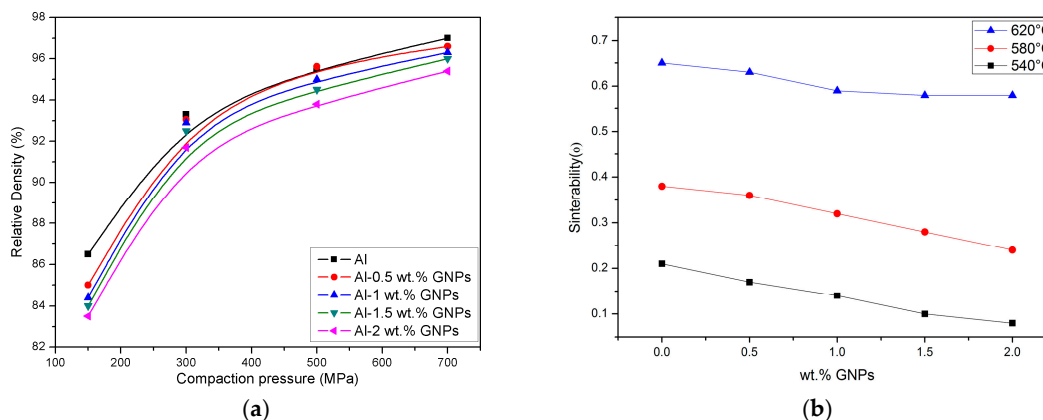


**Figure 7.** (a) Consolidation curve and (b) sinterability curves of Al/GNPs nanocomposites as a function of GNPs [130], Reproduced from [130], with permission from Springer Nature, 2017.

Saboori et al. have also studied the effect of graphene addition on the Vickers hardness and thermal conductivity of Al/GNPs nanocomposites (Figure 8a,b) [129]. The most interesting finding in their work was thermal conductivity improvement at low graphene content and lower thermal conductivity at higher graphene content. Then this significant discrepancy was correlated to the GNPs agglomeration formation at higher graphene content. Moreover, in Figure 8b there is a clear trend of increasing the Vickers hardness by increasing the graphene content. Nonetheless, it should be noted that even in this case the Vickers hardness of nanocomposites at a higher GNPs content is deteriorated as a consequence of GNPs agglomeration.

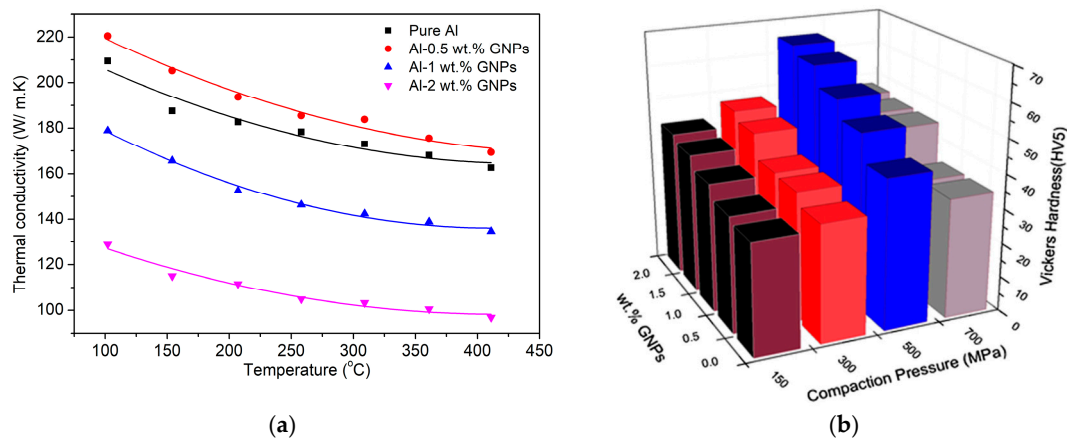


**Figure 8.** (a) Thermal conductivity and (b) Vickers hardness of Al/GNPs nanocomposites as a function of GNPs [129], Reproduced from [129], with permission from Springer Nature, 2017.

In another work, Saboori et al. have compared the microstructure and thermal conductivity of Al/GNPs produced by conventional powder metallurgy and hot rolling [131]. The microstructural observations in this work showed that by increasing the graphene content, the number of GNPs agglomerates increases dramatically (Figure 9). All the graphene nanoplatelets were placed at the grain boundary that resulted in the grain refinement down to 6  $\mu\text{m}$  in the case of Al-1 wt % GNPs. The grain boundary observations in this work showed there were a lot of voids at the grain boundaries and so the interfacial grain boundary was not strong enough to improve the final properties. Regarding the Al/GNPs nanocomposites produced by hot rolling, it should be noticed that even in this case despite the consolidation using an external force, still there was not a strong interfacial bonding between the aluminum and GNPs (Figure 10). According to their thermal conductivity measurements, the thermal conductivity of Al/GNPs nanocomposites increased slightly and then decreased significantly as a consequence of graphene agglomeration and poor interfacial bonding (Figure 11). The most interesting aspect of this evaluation is in the comparison between the models and experimental results, and as can be seen in Figure 11, the experimental results were in the range of parallel model that confirms the presence of preferred orientation of GNPs within the matrix. Apart from the preferred orientation of GNPs and GNPs agglomerate formation, the higher thermal conductivity of samples produced by hot rolling was correlated to their higher density and lower porosity content.

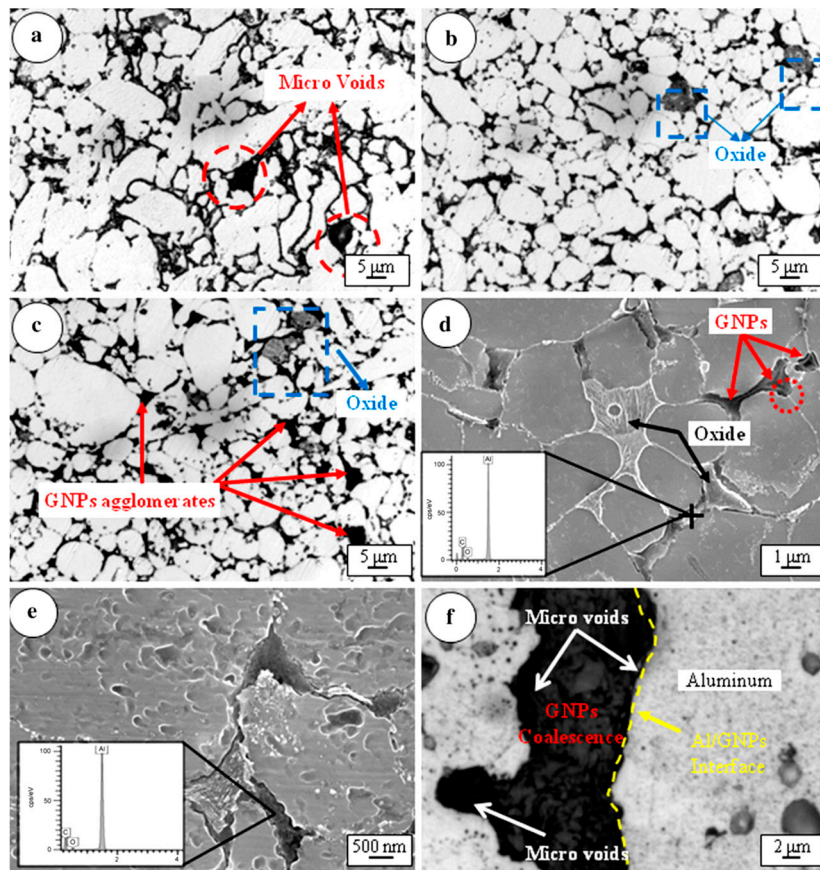


**Figure 9.** Optical microscopy (OM) micrograph of press-sintered (a) pure Al, (b) Al-0.5 wt % GNPs, (c) Al-1.0 wt % GNPs, (d) scanning electron microscopy (SEM) image of Al-1.0 wt % GNPs, (e) EDS analysis at a grain boundary, (f) a representative grain boundary of Al-1.0 wt % GNPs after sintering [131], Reproduced from [131], with permission from Springer Nature, 2017.

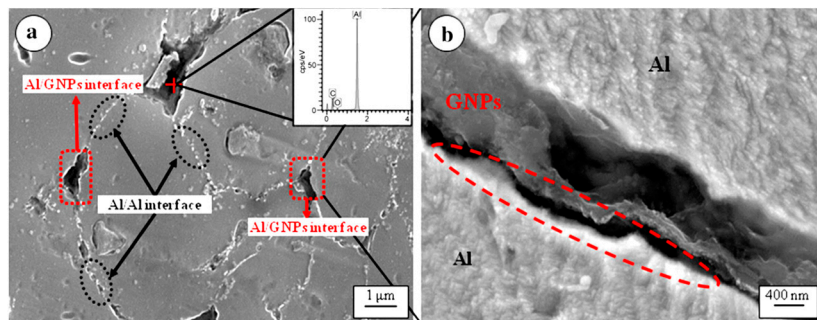


**Figure 10.** SEM micrograph of (a) hot-rolled Al-1.0 wt % GNPs, (b) magnification of an Al/GNPs interface [131], Reproduced from [131], with permission from Springer Nature, 2017.

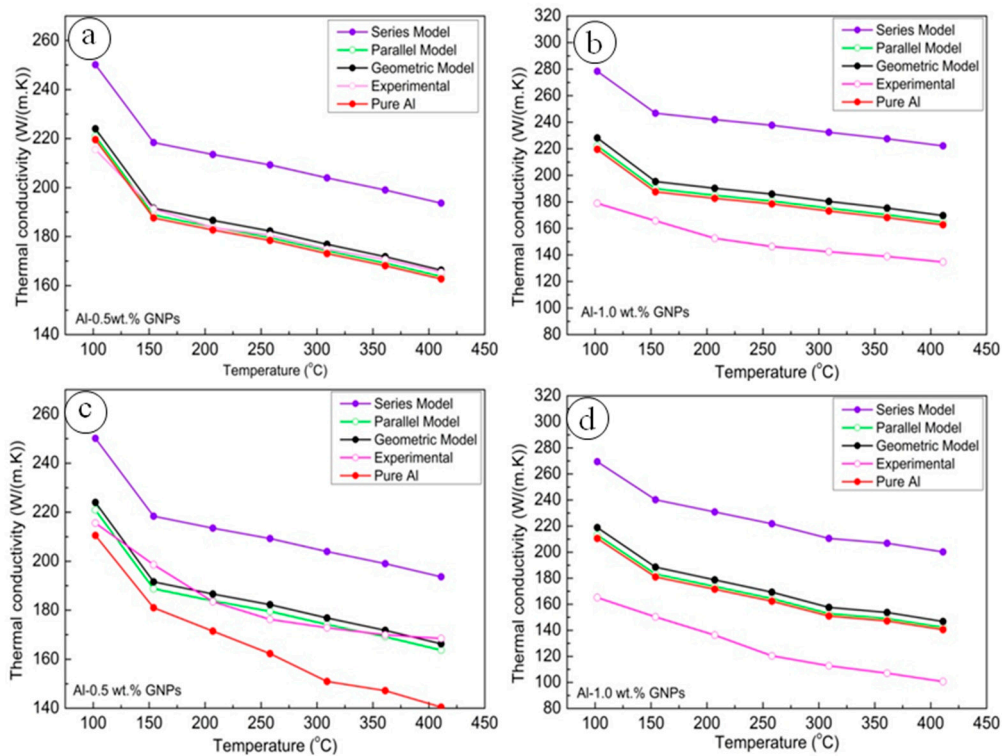


**Figure 11.** The thermal conductivity of Al/GNPs nanocomposites produced by (a,b) press-sintering process, (c,d) hot rolling [131], Reproduced from [131], with permission from Springer Nature, 2017.

Recently, Saboori et al. have studied the effect of graphene addition on microstructure and mechanical properties of AlSi10Mg/GNPs nanocomposites produced by hot extrusion [132]. In this research, AlSi10Mg composites reinforced with graphene nanoplatelets (GNPs) were produced by a wet mixing method followed by two-step hot consolidation (hot compaction then hot extrusion) at 400 °C. The weight percentages of GNPs were 0.5 and 1 wt % concerning the AlSi10Mg alloy. Tensile and Vickers hardness tests at room temperature were performed to evaluate the effect of GNPs on mechanical properties of the as-fabricated composite. The outcomes show that the high quantity of GNPs (>0.5 wt %) deteriorates the mechanical properties of AlSi10Mg composite due to the agglomeration of GNPs and, as a consequence, introduction of internal porosity in the composite. However, it is found that relatively low fraction of GNPs can uniformly be dispersed in the Al alloy matrix through the wet mixing method. The hardness and tensile results demonstrated that the mechanical properties improve slightly through the addition of 0.5 wt % of GNPs, while 1.0 wt % GNPs addition did not lead to improved performance owing to overwhelming effects of porosity (Figure 12).

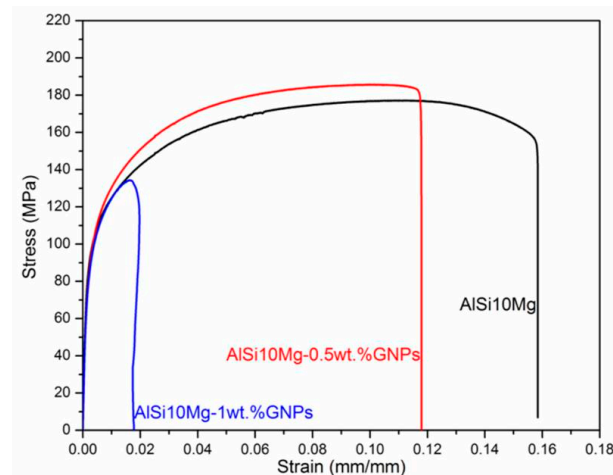


**Figure 12.** Tensile stress-strain curves of AlSi10Mg/GNPs curves produced by hot rolling [132], Reproduced from [132], with permission from Springer Nature, 2018.

### 5. Copper Matrix Composites (CuMCs)

These days, electronic devices due to their high performance and packing density release much more heat concerning the earlier devices. Thus, thermal management becomes a considerable issue that should be addressed in order to increase the performance of the new devices. Heat sinks which are the cooling systems for the electronic devices have been developed to solve this issue. In fact, a heat sink should transfer the heat fluxes to the cooling media in order to manage the released heat. Copper and copper composites are very interesting materials that can be used in this application due to their promising features such as high thermal conductivity and low electrical resistance. However, in order to develop the application of copper composites, it is necessary to fabricate new composites with high thermal conductivity, high electrical conductivity, low coefficient of thermal expansion and high mechanical properties. Thus, it is essential to design the material to have a uniform dispersion of reinforcing material as well as a strong interfacial bonding between the reinforcement and matrix. Copper matrix composites can be produced by the addition of stable and non-soluble particles into the copper matrix. These non-soluble and stable particles can be different based on the target application, and they could be oxides ( $\text{Al}_2\text{O}_3$ ,  $\text{SiO}_2$ , etc.), borides ( $\text{TiB}_2$ ,  $\text{ZrB}_2$ , etc.), nitrides ( $\text{TiN}$ ,  $\text{ZrN}$ , etc.), carbides ( $\text{SiC}$ ,  $\text{B}_4\text{C}$ ,  $\text{TiC}$ , etc.) and carbonaceous materials (CNTs, graphite, graphene, diamond) [133–135]. Among the oxides which are the best reinforcing materials regarding mechanical properties due to their high hardness and stability, copper oxide and nickel oxide are not stable at high temperatures and cannot be a suitable reinforcement for the high-temperature applications [136]. According to the literature, due to the poor wettability between the molten copper and reinforcing particles conventional casting techniques are not appropriate fabrication techniques for this kind of composites. Thus, other manufacturing routes such as powder metallurgy techniques are developed to produce the copper-based composites [135]. The level of porosity in the copper-based composites has different effects in various applications in such a way that in the electronic packaging it has a negative effect whereas in self-lubrication bearings or filters has a positive effect and can act as oil reservoirs [135]. However, there is a large volume of published studies describing the role of different reinforcements on mechanical and thermal properties of the CuMCs and some of the recent efforts are listed in Table 3. The main areas of interest for copper and its composites are the electronic packaging and heatsink industries as well as the structural and frictional applications [135,137,138]. It should be noticed that the electrical properties of copper composites can be affected seriously by the impurities so that some of them may precipitate during the heat treatment and these formed precipitates deteriorate the electrical conductivity [137]. For instance, Caron et al. have reported that the electrical conductivity of copper can be lower down to 86% IACS (International Annealed Copper

Standard) only as a consequence of 0.023% Fe addition during the fabrication process [137]. Moreover, it is reported that the presence of 0.3% Zr, 1.25% Al, 0.1% P can lower the electrical conductivity of copper to 85%, 70% and 50% IACS, respectively [135].

In order to broaden the application of copper composites in the electrical contact parts like high-voltage switches, rocket nozzle liners, spot welding electrodes several unique features are required. These essential properties can be 140 HV in hardness, the thermal conductivity of 320 W/m·K and electrical conductivity of 80% IACS. Having high mechanical strength together with high thermal and electrical conductivities is almost puzzling for copper composites so that in most cases improving the mechanical properties sacrifices the thermal and electrical properties of the composites and it is necessary to find an appropriate balance between these properties. Zhao et al. have prepared a copper matrix composite reinforced by Ni coated CNTs by the combination of conventional powder metallurgy followed by forging and die stretching. They found that the CNTs were aligned along the stretching direction and the hardness and tensile strength of the composite were improved remarkably up to 67% and 30%, respectively, with respect to the pure copper. They have seen anisotropic characteristics in thermal and electrical conductivity as well as mechanical properties of the composites [139].

**Table 3.** A summary of recent research on CuMCs reinforced by carbon allotropes.

Matrix	Reinforcement <sup>a</sup>	Content (wt %)	Fabrication Technique <sup>b</sup>	Properties <sup>c</sup>	Ref.
Cu	GNPs	0.5	In-situ CVD	TS: 308 MPa	[19]
Cu	Graphene	0.5	CPM + HP	HV: 97 EC: 96% IACS	[2]
Cu	Graphite	0.5	CPM + HP	HV: 94 EC: 75% IACS	[2]
Cu	Graphene	0–4 vol %	SPS	E: 90–140 MPa Hardness: 1–1.8 GPa EC: 80–92% IACS	[21]
Cu	GNSs	0.5	BM + HP	TS: 120–220 MPa HV: 37–52	[22]
Cu	SWCNTs	5 vol %	CPM + Forging	TS: 274 MPa HV: 60 EC: 44–48% IACS TC: 310–378 W/m·K	[139]
Cu	Graphite	0.1	Roll-bonding	HV: 110–160 EC: 90–99% IACS	[140]
Cu	CNTs	0.5 vol %	SPS + wire drawing	TS: 558 MPa EC: 91.2% IACS	[141]

<sup>a</sup> CNTs: Carbon Nanotubes, GNSs: Graphene Nanosheets, GNPs: Graphene Nanoplatelets; <sup>b</sup> CPM: Conventional Powder Metallurgy, HP: Hot Press, SPS: Spark Plasma Sintering; <sup>c</sup> ST: Tensile strength, EC: Electrical conductivity, E: Elastic modulus, TC: Thermal conductivity.

Chen et al. have fabricated a copper/graphene nanocomposite by in-situ CVD followed by hot pressing. They found that a uniform dispersion of graphene, as well as desirable interfacial bonding, can be obtained by this technique which can result in a significant improvement in mechanical properties [19]. In addition, Zhang et al. have prepared graphene-copper composite through a semi-powder method and studied the mechanical properties of the composite. In this work, electroless copper and nickel were carried out on the surface of the graphene to improve the wettability of the graphene. According to their results, the yield strength of the composite was increased up to 49% and 64% for the copper coated and nickel coated graphene/copper composites with respect to the pure copper, and that could be a consequence of the formation of a strong interfacial bonding with the matrix. Thus, it is clear that the interfacial bonding plays a key role in the final mechanical and thermal properties of the composite and it needs to be designed carefully to achieve the full potential of the reinforcement. Saboori et al. have produced Cu-GNPs nanocomposites using

conventional powder metallurgy followed by repress-annealing and Hot isostatic pressing (HIP) processes as post processes [142]. In this work, the effect of some post-processing on the thermal conductivity of nanocomposites has been investigated (Figure 13). As it can be seen in Figure 13, the thermal conductivity of pure copper and Cu-8 wt % GNPs increased after repressing-annealing and hot isostatic pressing and this increment were correlated to the reduction of porosity using those post-processing techniques. Moreover, it is clear that the efficiency of the HIP in the reduction of porosity and accordingly thermal conductivity was higher than repressing and annealing. Figure 14 compares the experimental thermal conductivity of Cu/GNPs nanocomposite with the theoretical models. From these graphs it could be understood two main effects of graphene nanoplatelets; (I) lower GNPs contents resulted in thermal conductivity improvement and higher GNPs content deteriorate this feature, (II) Preferred orientation of GNPs resulted in the anisotropic thermal conductivity of nanocomposites.

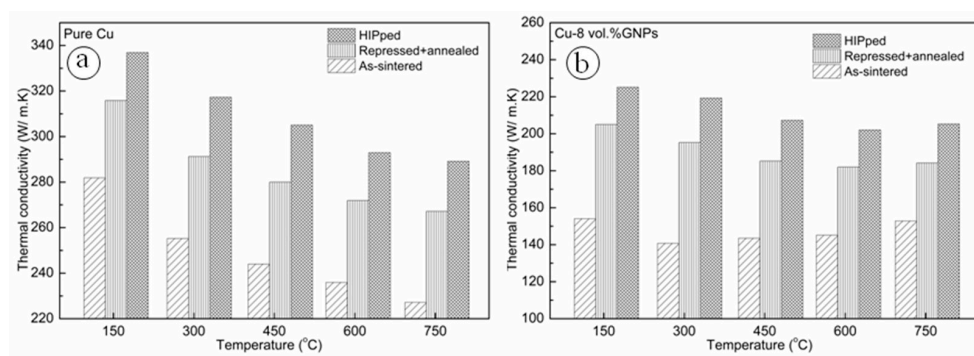


**Figure 13.** conductivity of (a) pure Cu, (b) Cu-8 vol % GNPs after sintering, repressing-annealing and HIPping processes [142], Reproduced from [142], with permission from Springer Nature, 2018.

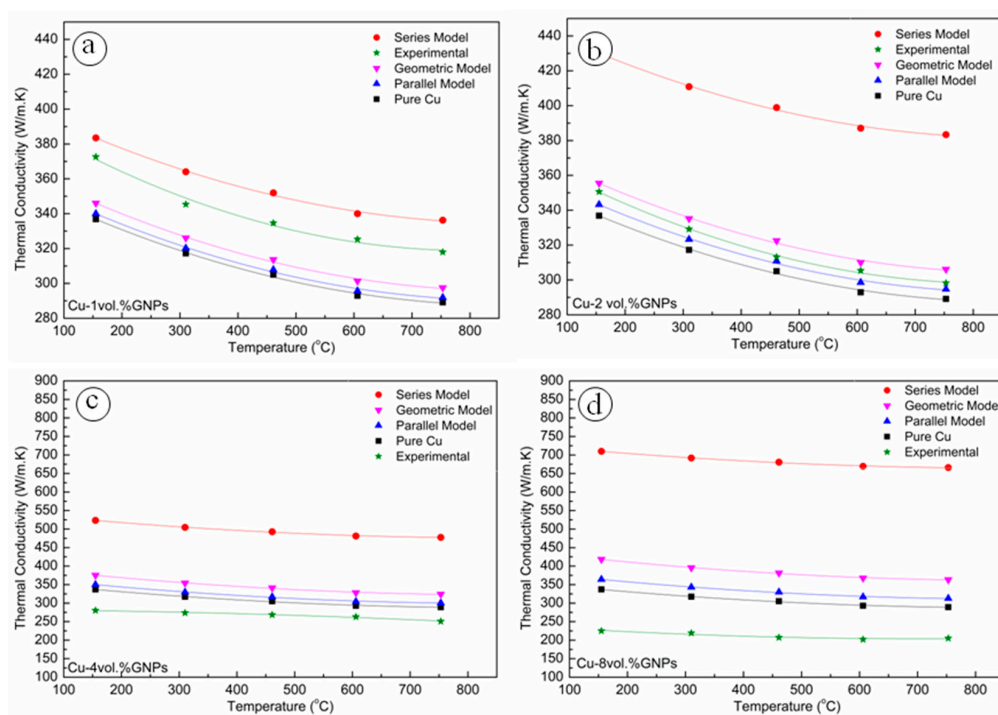


**Figure 14.** Comparison of experimental thermal conductivities of (a) Cu-1 vol % GNPs, (b) Cu-2 vol % GNPs, (c) Cu-4 vol % GNPs, (d) Cu-8 vol % GNPs, to the prediction by different models [142], Reproduced from [142], with permission from Springer Nature, 2018.

In other research, Saboori et al. have investigated the effect of GNPs on the mechanical strength, coefficient of thermal expansion of Cu/GNPs nanocomposites [143]. In this work, it is shown that through the addition of GNPs it would be possible to address the main disadvantage of copper for the electro-packaging industries and reduce the coefficient of thermal expansion of copper up to 40% (Figure 15). Moreover, the experimental CTEs were compared with the theoretical numbers, and it is reported that through the preferential orientation of GNPs it would be possible to decrease the CTE of the copper nanocomposites.

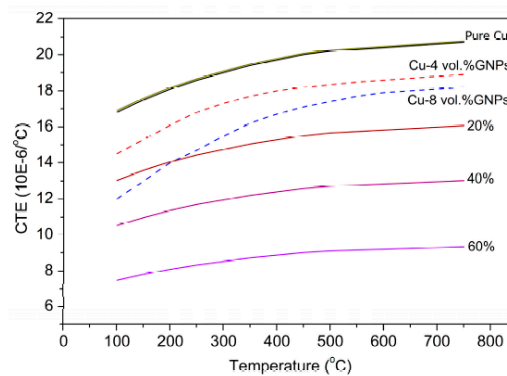


**Figure 15.** The theoretical predictions and experimental coefficient of thermal expansion of pure copper, Cu-4 vol % GNPs, and Cu-8 vol % GNPs as a function of temperature [142], Reproduced from [142], with permission from Springer Nature, 2018.

Chu et al. have studied the mechanical properties of Cu/GNPs nanocomposites with randomly distributed graphene [144]. In this work, it was attempted to align graphene nanoplatelets (GNPs) in the copper matrix using a vacuum filtration technique followed by spark plasma sintering (SPS). It was revealed that a fairly good graphene alignment was obtained and this alignment resulted in the prominent anisotropic mechanical performance with in-plane tensile strength and elongation significantly outperforming through-plane ones. Nonetheless, only moderate in-plane strength improvement (26% at 10 vol % GNPs) was achieved in the composites, and this achievement was further diminished to  $-7.1\%$  with increasing GNP content to 20 vol %, which was related primarily to the weak GNP-Cu (Figure 16). Moreover, the anisotropic mechanical behavior of aligned Cu/GNP composites was proposed to originate from the different interface failure modes of ‘GNP slippage’ and ‘GNP peer-off’ with the load parallel and perpendicular to the alignment direction, respectively.

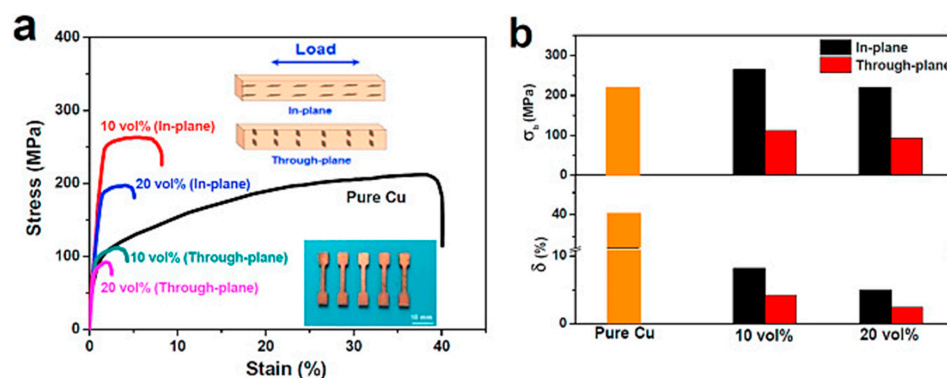


**Figure 16.** (a) Tensile stress-strain curves and (b) obtained properties of tensile strength ( $\sigma_b$ ) and elongation ( $\delta$ ) for pure Cu and 10 vol %/20 vol % GNP/Cu composites with the load parallel and perpendicular to the alignment direction [144], Reproduced from [144], with permission from Elsevier, 2018.

Consolidation of copper matrix nanocomposites was found to be one of the challenges that can dramatically affect the final properties of the nanocomposites. For this reason, Saboori et al. have studied the effect of some post-processing techniques such as repressing-annealing and hot isostatic pressing on the final porosity content, density, electrical conductivity and interfacial bonding of copper/graphene [10]. Figure 17 compares the theoretical, as-sintered, repressed-annealed and HIPed density of Cu/GNPs nanocomposites. As can be seen, the lowest density is related to as-sintered Cu/GNPs nanocomposites and this density increased by using the post-processing step. Between the post-processing methods, HIPing showed great potential in porosity elimination after sintering and thus it can be used as a proper post-processing technique.

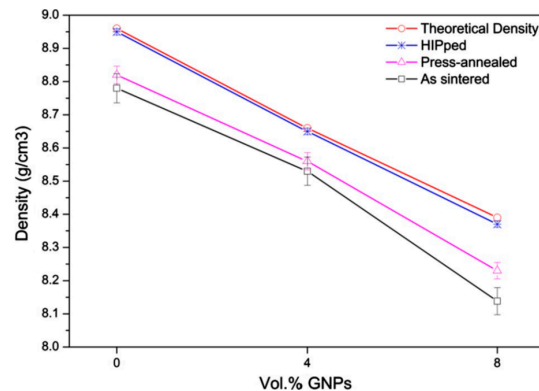


**Figure 17.** Theoretical and measured densities of composites after sintering and two different post-processing techniques (repressing followed by annealing and HIPing) [10], Reproduced from [10], with permission from Springer Nature, 2018.

Figure 18 compares the interface of Cu/GNPs after sintering and sintering followed by annealing by means of field emission scanning electron microscopy (FESEM) images. As it can be seen, the interfacial bonding in the as-sintered sample is very weak and consists of lots of porosity at the interface while; there is no porosity at the interface of Cu/GNPs after HIPing that results in the formation of strong interfacial bonding between Cu and GNPs.

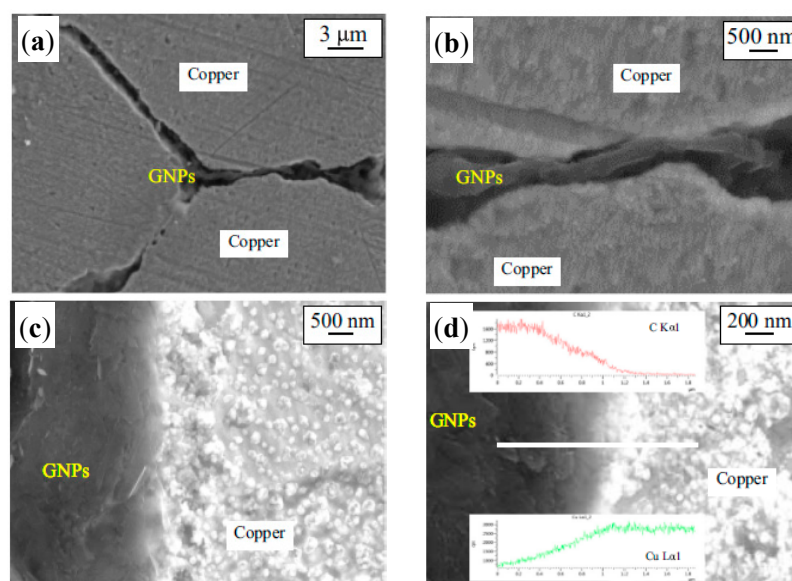


**Figure 18.** FESEM images of the interface between Cu and GNPs in the (a,b) as-sintered, and (c,d) HIPed specimens [10], Reproduced from [10], with permission from Springer Nature, 2018.

The electrical conductivity of Cu/GNPs nanocomposites after HIPing were compared with as-sintered ones, and it is reported that after HIPing when the porosity content of Cu/GNPs nanocomposites decreases, the electrical conductivity of nanocomposites significantly increases. Table 4 summarizes the electrical conductivity of Cu/GNPs nanocomposites produced by different techniques. According to this table, it can be concluded that the fabrication process, type quality and the weight percentage of reinforcement play key roles in the electrical conductivity of Cu composites.

**Table 4.** A summary of the electrical conductivity reports for Cu-GNPs composites.

Reinforcement	Content	Electrical Conductivity (%IACS)	Fabrication Method	Ref.
MLG	1–5 wt %	78.5–61.5	Flake PM	[145]
CNT	1–5 wt %	74.6–5.3	Flake PM	[146]
Nano-Graphite	1–5 wt %	78.5–68.3	Flake PM	[49]
CNTs	0.5 vol %	91.2	SPS + wire drawing	[141]
GNPs	0.6 vol %	88	Molecular level mixing + SPS	[21]
Graphite	8.0 wt %	55	Cu coating of graphene + sintering	[147–149]
Graphite	0.1 vol %	90%	Roll bonding	[140]
-	-	52.3	Sintering + Forging	[139]
SWCNTs	5 vol %	44.5	Sintering + Forging	[10]
-	-	78	Sintering + HIPping	[10]
GNPs	2 vol %	77	Sintering + HIPping	[10]
GNPs	4 vol %	72.5	Sintering + HIPping	[10]
GNPs	8 vol %	67.5	Sintering + HIPping	[10]

## 6. Magnesium Matrix Composites (MgMCs)

Magnesium matrix composites reinforced by short fibers were developed firstly in the 1980s, but reinforcing with nanoparticles is of great of interest in recent research on magnesium matrix composites. As a matter of fact, this increasing trend of using the nanoparticles in MMNCs is due this fact that by using small amount of nanoparticles, it would be possible to achieve a noticeable improvement in the mechanical properties of the composite [56,147]. Due to the unique features of magnesium such as low density and high specific strength, these nanocomposites could attract more attention in the academia and industries. In particular, in the automotive and aerospace industries there is a great interest in magnesium alloys in order to use these alloys to reduce their vehicle's weight and consequently reduce the fuel consumption and CO<sub>2</sub> emission. Nonetheless, some poor features of magnesium alloys like, poor creep properties, low modulus, low strength at elevated temperatures are limiting their applications. Thus, magnesium matrix composites reinforced by nanoparticles have been developed to address the aforementioned drawbacks and broaden the applications of the magnesium matrix composites. Silicon carbide (SiC), titanium carbide (TiC) and aluminum nitride (AlN) and aluminum oxide (Al<sub>2</sub>O<sub>3</sub>) are the most common reinforcements used in magnesium matrix composites [150]. In fact, reinforcing the Mg matrix composites by SiC particles leads to a noticeable improvement in their mechanical properties such as ultimate tensile strength, hardness, and ductility as well as in their wear resistance. On the other hand, TiC particles can improve the mechanical properties of the composite as well as their damping capacity while, their ductility would be deteriorated. Aluminum oxide particles can affect the creep resistance and compressive strength of magnesium-based composites positively. B<sub>4</sub>C particles, as reinforcement in the magnesium matrix composites improve the interfacial bonding, flexural strength and wear resistance [150,151]. Recently, Xiuqing and coworkers have investigated the effect of TiB<sub>2</sub> + TiC addition on the mechanical properties of pure magnesium and thereafter they have compared the obtained results with the AZ91 magnesium alloy after heat treatment. They found that the tensile properties of Mg/TiB<sub>2</sub> + TiC were remarkably better than those of heat-treated AZ91 magnesium alloy, whereas the ductility of the composite was worse than AZ91 after heat treatment [152]. Hou et al. have studied the effect of Ni-coated short carbon fiber on the thermal and mechanical properties of magnesium composites. They have reported that the

hardness and compressive strength improvement were obtained in the case of composite as well as the grain refinement. They also showed that it would be possible to achieve a balance between appropriate mechanical properties and thermal conductivity of composite, simultaneously [153]. Suresh et al. have studied the effect of charcoal addition on ageing response of AZ91 magnesium alloy. They have shown that a significant grain refinement can be obtained through the addition of only 0.2 wt % charcoal and this grain refinement is occurred as a consequence of  $Al_4C_3$  and  $Al_2MgC_2$  particles formation during melting. Moreover, they have shown that the addition of charcoal can increase the ageing rate and it would be possible to reach the maximum hardness at shorter periods [154]. Rashad et al., have fabricated Mg-Al-graphene nanoplatelets (GNPs) nanocomposites using the powder metallurgy method. In this work, the effect of Al-GNPs hybrids addition in to pure Mg was evaluated via tensile and Vicker hardness tests [155]. The GNPs content was kept constant (0.18 wt %) and Al content was varied from 0.5 wt % to 1.5 wt %. The increase in Al content resulted in increase in 0.2% YS, UTS and failure strain (%). However for Al content exceeding over 1 wt %, the failure strain (%) started to decrease. The best improvement was obtained with 1 wt % Al (Mg-1.0Al-0.18GNPs) (Figure 19). The mechanical strength of synthesized composites proved to be better than Mg-Al-CNTs and Mg-ceramic composites.

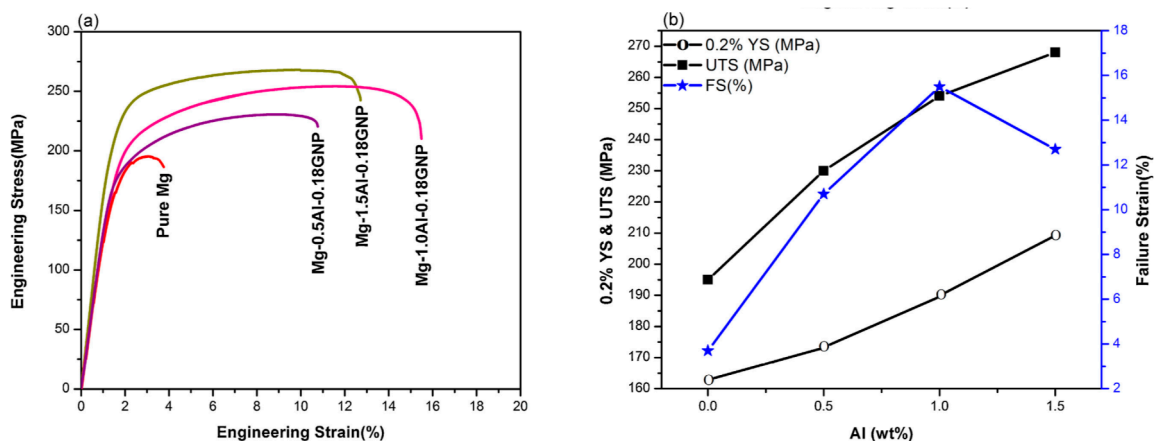


**Figure 19.** Tensile test of pure Mg and Mg- $x$ Al-0.18GNP composites ( $x = 0.5; 1.0; 1.5$ ) [155], Reproduced from [155], with permission from Springer Elsevier, 2015.

Rashad et al. have produced the Mg-1%Al-1%Sn-0.18%-graphene nanoplatelets (GNPs) composite by a semi powder metallurgy method followed by hot extrusion [1]. Microscopic evaluations revealed the homogeneous dispersion of GNPs in the matrix. The addition of 0.18 wt % GNPs to Mg-1 wt % Al-1 wt % Sn alloy increased tensile strength (i.e., from 236 to 269 MPa) (Figure 20). The increase in strength of the composite was correlated to the high specific surface area, superior nanofiller adhesion and two-dimensional structure of GNPs.

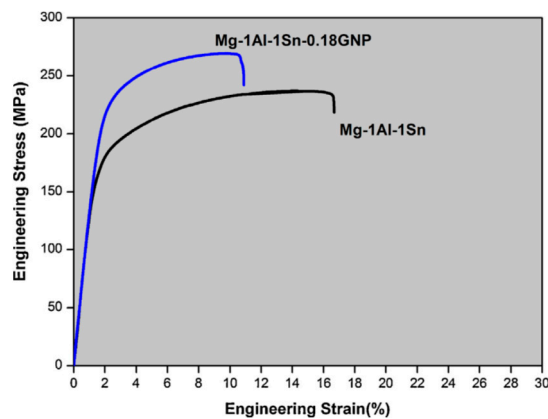


**Figure 20.** Tensile test of Mg-1Al-1Sn and Mg-1Al-1Sn-0.18GNP composites [1], Reproduced from [1], with permission from Elsevier, 2014.

Table 5 compares the mechanical properties of pure Mg, Mg alloys and Mg-based composites. As it can be seen Mg-Al-GNPs composites showed tensile strength and failure strain values higher than Mg-Al-CNT composites. This higher mechanical properties of Al-GNPs nanocomposites over Al-CNTs nanocomposites can be attributed to the high specific surface area, superior nanofiller matrix adhesion ascending from the crumpled surface, along with the two-dimensional (planar) structure of graphene nanoplatelets [156]. On the other hand, the one-dimensional structure of CNTs leads to the agglomerate formation, which resulted in lower the mechanical strength and failure strain (%) as a consequence of poor dispersion in the matrix [157]. Furthermore, it can be seen that Mg-Al-GNPs composites exhibited higher mechanical properties with respect to the composites reinforced with the high volume fraction of Ti, Al<sub>2</sub>O<sub>3</sub>, Cu and SiC particle hybrids. This comparison shows that small amount of inclusions is advantageous because it does not affect the lightweight properties of the Mg.

**Table 5.** Comparison of mechanical properties of Mg-based composites.

Materials	0.2% YS (MPa)	UTS (MPa)	Failure Strain (%)	Ref.
Pure Mg	162	195	3.7	[155]
Mg-1.0Al-1.0Sn	161	236	16.7	[1]
Mg-0.5Al-0.18GNPs	173	230	10.7	[155]
Mg-1.0Al-0.18GNPs	190	254	15.5	[155]
Mg-1.5Al-0.18GNPs	209	268	12.7	[155]
Mg-1.0Al-1.0Sn-0.18GNPs	208	268	10.9	[1]
Mg-1.5Al-0.18CNTs	156	223	7	[158]
Mg-5.6Ti-2.5Al <sub>2</sub> O <sub>3</sub>	168	214	6.8	[159]
Mg-1Al <sub>2</sub> O <sub>3</sub> -0.9Cu	202	232	4.1	[160]
Mg-5.6Ti-3Cu	197	225	2.6	[161]
Mg-21.3SiC	128	176	1.4	[162]
AZ91-10SiC	120	135	0.47	[163]

## 7. Conclusions

It is found that through the introduction of GNPs into a metallic matrix, some properties such as mechanical characteristics, and thermal and electrical conductivities can be improved simultaneously with reduction of coefficients of thermal expansion. However, it should be mentioned there are several technical challenges in the fabrication of metal matrix composites, such as (I) reinforcement selection, (II) reinforcement dispersion, (III) reactivity between the reinforcement and matrix, (IV) interfacial bonding, and (V) preferred orientation of reinforcement. To benefit from the excellent features of the reinforcement within the metallic matrix, these technical challenges should be addressed before or within the fabrication process. A uniform dispersion of GNPs within these matrices can be achieved

via powder metallurgy and laser-based 3D printing technologies. In general, it is found that the thermal conductivity and mechanical properties of composites depend strongly on the graphene content, dispersing of graphene, and interfacial bonding between graphene and metallic matrices. Low graphene contents lead to the improvement of properties, and higher graphene contents deteriorate the properties of composites, mainly because of graphene agglomerate formation. The residual porosity content can be reduced using some post-processing techniques. This porosity elimination results in the improvement of interfacial bonding and consequently properties of composites. During the fabrication of MMNCs, graphene nanoplatelets are mainly located at the grain boundaries and lead to grain refinement, which is the main strengthening source. The preferred orientation of GNPs during the compaction leads to the anisotropic properties of composites. Due to the high specific surface area, superior nanofiller matrix adhesion ascending from the crumpled surface, along with the two-dimensional (planar) structure of graphene nanoplatelets, the mechanical properties of Al-GNPs nanocomposites are higher than Al-CNT nanocomposites. All in all, it can be concluded that despite a lot of challenges that are present in the fabrication of MMNCs reinforced by GNPs, it would be possible to produce new metal matrix nanocomposites with superior thermal and mechanical properties as well as lower coefficient thermal expansion.

**Author Contributions:** Indeed in this review, A.S. and M.D. searched in the literature to find the proper research and published works and wrote the paper. P.F. and M.P. reviewed the paper.

**Funding:** This research received no external funding.

**Conflicts of Interest:** The authors declare no conflict of interest.

## References

1. Rashad, M.; Pan, F.; Asif, M.; Tang, A. Powder metallurgy of Mg–1% Al–1% Sn alloy reinforced with low content of graphene nanoplatelets (GNPs). *J. Ind. Eng. Chem.* **2014**, *20*, 4250–4255. [[CrossRef](#)]
2. Wang, X.; Li, J.; Wang, Y. Improved high temperature strength of copper-graphene composite material. *Mater. Lett.* **2016**, *181*, 309–312. [[CrossRef](#)]
3. Wang, J.; Li, Z.; Fan, G.; Pan, H.; Zhang, D. Reinforcement with graphene nanosheets in aluminum matrix composites. *Sci. Mater.* **2012**, *66*, 594–597. [[CrossRef](#)]
4. Jeon, C.-H.; Jeong, Y.-H.; Seo, J.-J.; Tien, H.N.; Hong, S.-T.; Yum, Y.-J.; Hur, S.-H.; Lee, K.-J. Material properties of graphene/aluminum metal matrix composites fabricated by friction stir processing. *Int. J. Precis. Eng. Manuf.* **2014**, *15*, 1235–1239. [[CrossRef](#)]
5. Perez-Bustamante, R.; Bolanos-Morales, D.; Bonilla-Maetinez, J.; Estrada-Guel, I. Microstructural and hardness behavior of graphene-nanoplatelets aluminum composites synthesized by mechanical alloying. *J. Alloys Compd.* **2014**, *615*, S578–S582. [[CrossRef](#)]
6. Saboori, A.; Padovano, E.; Pavese, M.; Badini, C. Novel magnesium Elektron21-AlN nanocomposites produced by ultrasound-assisted casting; microstructure, thermal and electrical conductivity. *Materials* **2018**, *11*, 27. [[CrossRef](#)] [[PubMed](#)]
7. Saboori, A.; Dadkhah, M.; Pavese, M.; Manfredi, D.; Biamino, S.; Fino, P. Hot deformation behavior of Zr-1% Nb alloy: Flow curve analysis and microstructure observations. *Mater. Sci. Eng. A* **2017**, *696*, 366–373. [[CrossRef](#)]
8. Tabandeh-Khorshid, M.; Omrani, E.; Menezes, P.L.; Rohatgi, P.K. Tribological performance of self-lubricating aluminum matrix nanocomposites: Role of graphene nanoplatelets. *Eng. Sci. Technol. Int. J.* **2016**, *19*, 463–469. [[CrossRef](#)]
9. Saboori, A.; Pavese, M.; Biamino, S.; Fino, P.; Lombardi, M. Determination of critical condition for initiation of dynamic recrystallisation in Zr-1% Nb alloy. *J. Alloys Compd.* **2018**, *757*, 1–7. [[CrossRef](#)]
10. Saboori, A.; Pavese, M.; Badini, C.; Fino, P. A Novel Approach to enhance the mechanical strength and electrical and thermal conductivity of Cu-GNP nanocomposites. *Metall. Mater. Trans. A Phys. Metall. Mater. Sci.* **2018**, *49*. [[CrossRef](#)]

11. Moghadam, A.D.; Omrani, E.; Menezes, P.L.; Rohatgi, P.K. Mechanical and tribological properties of self-lubricating metal matrix nanocomposites reinforced by carbon nanotubes (CNTs) and graphene—A review. *Compos. Part B Eng.* **2015**, *77*, 402–420. [[CrossRef](#)]
12. Saboori, A.; Padovano, E.; Pavese, M.; Dieringa, H.; Badini, C. Effect of solution treatment on precipitation behaviors, age hardening response and creep properties of Elektron21 alloy reinforced by AlN nanoparticles. *Materials* **2017**, *10*, 1380. [[CrossRef](#)] [[PubMed](#)]
13. Neubauer, E.; Kitzmantel, M.; Hulman, M.; Angerer, P. Potential and challenges of metal-matrix-composites reinforced with carbon nanofibers and carbon nanotubes. *Compos. Sci. Technol.* **2010**, *70*, 2228–2236. [[CrossRef](#)]
14. Saboori, A.; Pavese, M.; Badini, C.; Fino, P. Development of Al- and Cu-based nanocomposites reinforced by graphene nanoplatelets: Fabrication and characterization. *Front. Mater. Sci.* **2017**, *11*, 171–181. [[CrossRef](#)]
15. Saboori, A.; Gallo, D.; Biamino, S.; Fino, P.; Lombardi, M. An overview of additive manufacturing of titanium components by directed energy deposition: Microstructure and mechanical properties. *Appl. Sci.* **2017**, *7*, 883. [[CrossRef](#)]
16. Zhang, H.; Xu, C.; Xiao, W.; Ameyama, K.; Ma, C. Enhanced mechanical properties of Al5083 alloy with graphene nanoplates prepared by ball milling and hot extrusion. *Mater. Sci. Eng. A* **2016**, *658*, 8–15. [[CrossRef](#)]
17. Dieringa, H. Properties of magnesium alloys reinforced with nanoparticles and carbon nanotubes: A review. *J. Mater. Sci.* **2011**, *46*, 289–306. [[CrossRef](#)]
18. Ben-hamu, G.; Eliezer, D.; Shin, K.S.; Cohen, S. The relation between microstructure and corrosion behavior of Mg–Y–RE–Zr alloys. *J. Alloys Compd.* **2007**, *431*, 269–276. [[CrossRef](#)]
19. Chen, Y.; Zhang, X.; Liu, E.; He, C.; Han, Y.; Li, Q.; Nash, P.; Zhao, N. Fabrication of three-dimensional graphene/Cu composite by in-situ CVD and its strengthening mechanism. *J. Alloys Compd.* **2016**, *688*, 69–76. [[CrossRef](#)]
20. Yolshina, L.A.; Muradymov, R.V.; Korsun, I.V.; Yakovlev, G.A.; Smirnov, S.V. Novel aluminum-graphene and aluminum-graphite metallic composite materials: Synthesis and properties. *J. Alloys Compd.* **2016**, *663*, 449–459. [[CrossRef](#)]
21. Chen, F.; Ying, J.; Wang, Y.; Du, S.; Liu, Z.; Huang, Q. Effects of graphene content on the microstructure and properties of copper matrix composites. *Carbon N. Y.* **2016**, *96*, 836–842. [[CrossRef](#)]
22. Yue, H.; Yao, L.; Gao, X.; Zhang, S.; Guo, E.; Zhang, H.; Lin, X.; Wang, B. Effect of ball-milling and graphene contents on the mechanical properties and fracture mechanisms of graphene nanosheets reinforced copper matrix composites. *J. Alloys Compd.* **2017**, *691*, 755–762. [[CrossRef](#)]
23. Xue, C.; Bai, H.; Tao, P.F.; Wang, J.W.; Jiang, N. Thermal conductivity and mechanical properties of flake graphite/Al composite with a SiC nano-layer on graphite surface. *Mater. Des.* **2016**, *108*, 250–258. [[CrossRef](#)]
24. Gao, X.; Yue, H.; Guo, E.; Zhang, H.; Lin, X.; Yao, L.; Wang, B. Preparation and tensile properties of homogeneously dispersed graphene reinforced aluminum matrix composites. *Mater. Des.* **2016**, *94*, 54–60. [[CrossRef](#)]
25. Tian, W.; Li, S.; Wang, B.; Chen, X.; Liu, J.; Yu, M. Graphene-reinforced aluminum matrix composites prepared by spark plasma sintering. *Int. J. Miner. Met. Mater.* **2016**, *23*, 723–729. [[CrossRef](#)]
26. Lavagna, L.; Massella, D.; Pavese, M. Preparation of hierarchical material by chemical grafting of carbon nanotubes onto carbon fibers. *Diam. Relat. Mater.* **2017**, *80*, 118–124. [[CrossRef](#)]
27. Prasad, S.V.; Asthana, R. Aluminum metal–matrix composites for automotive applications: Tribological considerations. *Tribol. Lett.* **2004**, *17*, 445–453. [[CrossRef](#)]
28. Musfirah, A.H.; Jaharah, A.G. Magnesium and aluminum alloys in automotive industry. *J. Appl. Sci. Res.* **2012**, *8*, 4865–4875.
29. Kulekci, M.K. Magnesium and its alloys applications in automotive industry. *Int. J. Adv. Manuf. Technol.* **2008**, *39*, 851–865. [[CrossRef](#)]
30. Hu, H.; Yu, A.; Li, N.; Allison, J.E. Potential magnesium alloys for high temperature die cast automotive applications: A review. *Mater. Manuf. Process.* **2003**, *18*, 687–717. [[CrossRef](#)]
31. Macke, A.; Schultz, B.F. Metal matrix composites offer the automotive industry and opportunity to reduce vehicle weight, improve performance. *Adv. Mater. Process.* **2012**, *45*, 19–23.
32. Saboori, A.; Pavese, M.; Badini, C.; Eivani, A.R. Studying the age hardening kinetics of A357 aluminum alloys through the Johnson–Mehl–Avrami theory. *Met. Powder Rep.* **2017**, *72*, 420–424. [[CrossRef](#)]

33. Saboori, A.; Moheimani, S.K.; Dadkhah, M.; Pavese, M.; Badini, C.; Fino, P. An overview of key challenges in the fabrication of metal matrix nanocomposites reinforced by graphene nanoplatelets. *Metals* **2018**, *8*, 172. [[CrossRef](#)]
34. Metal Matrix Composite. Available online: [https://en.wikipedia.org/wiki/Metal\\_matrix\\_composite](https://en.wikipedia.org/wiki/Metal_matrix_composite) (accessed on 15 January 2018).
35. Kopeliovich, D. Metal Matrix Composites (Introduction). Available online: [http://www.substech.com/dokuwiki/doku.php?id=metal\\_matrix\\_composites\\_introduction](http://www.substech.com/dokuwiki/doku.php?id=metal_matrix_composites_introduction), (accessed on 15 January 2018).
36. Casati, R.; Vedani, M. Metal matrix composites reinforced by nano-particles—A review. *Metals* **2014**, *4*, 65–83. [[CrossRef](#)]
37. Chen, Z.-C.; Takeda, T.; Ikeda, K. Microstructural evolution of reactive-sintered aluminum matrix composites. *Compos. Sci. Technol.* **2008**, *68*, 2245–2253. [[CrossRef](#)]
38. Kopeliovich, D. Polymer Matrix Composites (Introduction). Available online: [http://www.substech.com/dokuwiki/doku.php?id=polymer\\_matrix\\_composites\\_introduction](http://www.substech.com/dokuwiki/doku.php?id=polymer_matrix_composites_introduction) (accessed on 15 January 2018).
39. Kopeliovich, D. Ceramic Matrix Composites (Introduction). Available online: [http://www.substech.com/dokuwiki/doku.php?id=ceramic\\_matrix\\_composites\\_introduction](http://www.substech.com/dokuwiki/doku.php?id=ceramic_matrix_composites_introduction) (accessed on 15 January 2018).
40. Callister, W.D. *Materials Science and Engineering—An Introduction*; John Wiley & Sons, Inc.: New York, NY, USA, 2007; ISBN 9780471736967.
41. Tang, Y.; Liu, L.; Li, W.; Shen, B.; Hu, W. Interface characteristics and mechanical properties of short carbon fibers/Al composites with different coatings. *Appl. Surf. Sci.* **2009**, *255*, 4393–4400. [[CrossRef](#)]
42. Włodarczyk-Fligier, A.; Dobrzański, L.A.; Kremzer, M.; Adamiak, M. Manufacturing of aluminium matrix composite materials reinforced by Al<sub>2</sub>O<sub>3</sub> particles. *J. Achiev. Mater. Manuf. Eng.* **2008**, *27*, 99–102.
43. Huber, T.; Degischer, H.P.; Lefrance, G.; Schmitt, T. Thermal expansion studies on aluminium-matrix composites with different reinforcement architecture of SiC particles. *Compos. Sci. Technol.* **2006**, *66*, 2206–2217. [[CrossRef](#)]
44. Huu, T.; Requena, G.; Degischer, P. Thermal expansion behaviour of aluminum matrix composites with densely packed SiC particles. *Compos. Part A* **2008**, *39*, 856–865. [[CrossRef](#)]
45. Jeyasimman, D.; Sivaprasad, K.; Sivasankaran, S.; Narayanasamy, R. Fabrication and consolidation behavior of Al 6061 nanocomposite powders reinforced by multi-walled carbon nanotubes. *Powder Technol.* **2014**, *258*, 189–197. [[CrossRef](#)]
46. Rashad, M.; Pan, F.; Tang, A.; Asif, M.; Aamir, M. Synergetic effect of graphene nanoplatelets (GNPs) and multi-walled carbon nanotube (MW-CNTs) on mechanical properties of pure magnesium. *J. Alloys Compd.* **2014**, *603*, 111–118. [[CrossRef](#)]
47. Nie, K.B.; Wang, X.J.; Xu, L.; Wu, K.; Hu, X.S.; Zheng, M.Y. Influence of extrusion temperature and process parameter on microstructures and tensile properties of a particulate reinforced magnesium matrix nanocomposite. *Mater. Des.* **2012**, *36*, 199–205. [[CrossRef](#)]
48. Gaspera, E.D.; Tucker, R.; Star, K.; Lan, E.H.; Ju, Y.S.; Dunn, B. Copper-based conductive composites with tailored thermal expansion. *ACS Appl. Mater. Interfaces* **2013**, *5*, 10966–10974. [[CrossRef](#)] [[PubMed](#)]
49. Varol, T.; Canakci, A. The effect of type and ratio of reinforcement on the synthesis and characterization Cu-based nanocomposites by flake powder metallurgy. *J. Alloys Compd.* **2015**, *649*, 1066–1074. [[CrossRef](#)]
50. Tang, Y.; Yang, X.; Wang, R.; Li, M. Enhancement of the mechanical properties of graphene–copper composites with graphene–nickel hybrids. *Mater. Sci. Eng. A* **2014**, *599*, 247–254. [[CrossRef](#)]
51. Rana, R.S.; Purohit, R.; Das, S. Review of recent Studies in Al matrix composites. *Int. J. Sci. Eng. Res.* **2012**, *3*, 1–16.
52. Saboori, A.; Pavese, M.; Badini, C.; Fino, P. Effect of sample preparation on the microstructural evaluation of Al–GNPs nanocomposites. *Met. Microstruct. Anal.* **2017**, *6*, 619–622. [[CrossRef](#)]
53. Hu, H.; Kong, J. Improved thermal performance of diamond-copper composites with boron carbide coating. *J. Mater. Eng. Perform.* **2014**, *23*, 651–657. [[CrossRef](#)]
54. Zhang, D.; Zhan, Z. Preparation of graphene nanoplatelets-copper composites by a modified semi-powder method and their mechanical properties. *J. Alloys Compd.* **2016**, *658*, 663–671. [[CrossRef](#)]
55. Kielbus, A.; Rzychon, T.; Przeliorz, R. DSC and microstructural investigations of the Elektron21 magnesium alloy. *Mater. Sci. Forum* **2010**, *642*, 1447–1452. [[CrossRef](#)]

56. Katsarou, L.; Mounib, M.; Lefebvre, W.; Vorozhtsov, S.; Pavese, M.; Badini, C.; Molina-aldareguia, J.M.; Cepeda, C.; MariaTeresa, P.P.; Dieringa, H. Microstructure, mechanical properties and creep of magnesium alloy Elektron21 reinforced with AlN nanoparticles by ultrasound-assisted stirring. *Mater. Sci. Eng. A* **2016**, *659*, 84–92. [[CrossRef](#)]
57. Chen, X. Fabrication and Properties of Particulate Reinforced Aluminum Matrix Composites by Spontaneous Infiltration. Ph.D. Thesis, Politecnico di Torino, Torino, Italy, 2013.
58. Zhu, J.; Wang, F.; Wang, Y.; Zhang, B.; Wang, L. Interfacial structure and stability of a co-continuous SiC/Al composite prepared by vacuum-pressure infiltration. *Ceram. Int.* **2017**, *43*, 6563–6570. [[CrossRef](#)]
59. Dorfman, S.; Fuks, D. Carbon diffusion in copper-based metal matrix composites. *Sens. Actuators A Phys.* **1995**, *51*, 13–16. [[CrossRef](#)]
60. Chu, K.; Jia, C.; Guo, H.; Li, W. On the thermal conductivity of Cu–Zr/diamond composites. *Mater. Des.* **2013**, *45*, 36–42. [[CrossRef](#)]
61. Lide, D.R. *Handbook of Chemistry and Physics*, 84th ed.; CRC Press: Boca Raton, FL, USA, 2003.
62. Nishida, Y. *Introduction to Metal Matrix Composites: Fabrication and Recycling*; Springer: Heidelberg, Germany, 2013.
63. Cardarelli, F. *Materials Handbook: A Concise Desktop Reference*; Springer: London, UK, 2008.
64. Srinivasan, M. *Non-Oxide Materials: Applications and Engineering*; Springer: Dordrecht, The Netherlands, 1996; pp. 3–42.
65. Safdari, M. A Computational and Experimental Study on the Electrical and Thermal Properties of Hybrid Nanocomposites Based on Carbon Nanotubes and Graphite Nanoplatelets. Ph.D. Thesis, Virginia Polytechnic Institute and State University, Blacksburg, VA, USA, 2012.
66. Novoselov, K.S.; Geim, A.K.; Morozov, S.V.; Al, E. Electric field effect in atomically thin carbon films. *Science* **2004**, *306*, 666–669. [[CrossRef](#)] [[PubMed](#)]
67. Kim, H.; Abdala, A.A.; Macosko, C.W. Graphene/polymer nanocomposites. *Macromolecules* **2010**, *43*, 6515–6530. [[CrossRef](#)]
68. Rollings, E.; Gweon, G.-H.; Zhou, S.Y.; Mun, B.S.; McChesney, J.L.; Hussain, B.S.; Fedorov, A.V.; First, P.N.; de Heer, W.A.; Lanzara, A. Synthesis and characterization of atomically thin graphite films on a silicon carbide substrate. *J. Phys. Chem. Solids* **2006**, *67*, 2172–2177. [[CrossRef](#)]
69. Wang, X.; You, H.; Liu, F.; Li, M.; Wan, L.; Li, S.; Li, Q.; Xu, Y.; Tian, R.; Yu, Z.; et al. Large-scale synthesis of few-layered graphene using CVD. *Chem. Vap. Depos.* **2009**, *15*, 5356. [[CrossRef](#)]
70. Kosynkin, D.V.; Higginbotham, A.L.; Sinitiskii, A.; Lomeda, J.R.; Dimiev, A.; Price, B.K.; Tour, J.M. Longitudinal unzipping of carbon nanotubes to form graphene Nanoribbons. *Nature* **2009**, *458*, 872–876. [[CrossRef](#)] [[PubMed](#)]
71. Shen, J.; Hu, Y.; Li, C.; Qin, C.; Shi, M.; Ye, M. Layer-by-Layer Self-Assembly of Graphene Nanoplatelets. *Langmuir* **2009**, *25*, 6122–6128. [[CrossRef](#)] [[PubMed](#)]
72. Jang, B.; Zhamu, A. Processing of nanographene platelets (NGPs) and NGP nanocomposites: A review. *J. Mater. Sci.* **2008**, *43*, 5092–5101. [[CrossRef](#)]
73. Fukushima, H.; Drzal, L.; Rook, B.; Rich, M. Thermal conductivity of exfoliated graphite nanocomposites. *J. Therm. Anal. Calorim.* **2006**, *85*, 235–238. [[CrossRef](#)]
74. Stankovich, S.; Dikin, D.A.; Dommett, G.H.B.; Kohlhaas, K.M.; Zimney, E.J.; Stach, E.A.; Piner, R.D.; Nguyen, S.T.; Ruoff, R.S. Graphene-based composite materials. *Nature* **2006**, *442*, 282–286. [[CrossRef](#)] [[PubMed](#)]
75. Solis-Fernandez, P.; Bissett, M.; Ago, H. Synthesis, structure and applications of graphene-based 2D heterostructures. *Chem. Soc. Rev.* **2017**, *46*, 4572–4613. [[CrossRef](#)] [[PubMed](#)]
76. Zhu, Y.; Ji, H.; Cheng, H.-M.; Ruoff, R.S. Mass production and industrial applications of graphene materials. *Natl. Sci. Rev.* **2018**, *5*, 90–101. [[CrossRef](#)]
77. Tung, T.T.; Nine, M.J.; Krebsz, M.; Pasinszki, T.; Coghlan, C.J.; Tran, D.N.; Losic, D. Recent advances in sensing applications of graphene assemblies and their composites. *Adv. Funct. Mater.* **2017**, *27*, 1702891. [[CrossRef](#)]
78. Kováčik, J.; Emmer, Š. Thermal expansion of Cu/graphite composites: Effect of copper coating. *Kov. Mater.* **2011**, *49*, 411–416.
79. Hale, D.K. The physical properties of composite materials. *J. Mater. Sci.* **1976**, *11*, 2105–2141. [[CrossRef](#)]
80. Turner, P.S. Thermal-expansion stresses in reinforced plastics. *J. Res. NBS* **1946**, *37*, 239–250. [[CrossRef](#)]

81. Hashin, Z.; Shtrikman, S. A variational approach to the theory of the elastic behaviour of multiphase materials. *J. Mech. Phys. Solids* **1963**, *11*, 127–150. [[CrossRef](#)]
82. Schapery, R.A. Thermal expansion coefficients of composite materials based on energy principles. *J. Compos. Mater.* **1968**, *2*, 380–404. [[CrossRef](#)]
83. Thermal Conductivity 2016. Available online: <https://en.wikipedia.org/wiki/Thermalconductivity> (accessed on 10 January 2018).
84. Kittel, C. *Introduction to Solid State Physics*; Wiley: Hoboken, NJ, USA, 2005.
85. Völklein, F.; Reith, H.; Cornelius, T.W.; Rauber, M.; Neumann, R. The experimental investigation of thermal conductivity and the Wiedemann–Franz law for single metallic nanowires. *Nanotechnology* **2009**, *20*, 325706. [[CrossRef](#)] [[PubMed](#)]
86. Davis, J.R. *Copper and Copper Alloys*; ASM International: Materials Park, OH, USA, 2001.
87. Boden, A. Copper Graphite Composite Materials—A Novel Way to Engineer Thermal. Ph.D. Thesis, Freien Universität Berlin, Berlin, Germany, 2015.
88. Klemens, P.G.; Pedraza, D.F. Thermal conductivity of graphite in the basal plane. *Carbon N. Y.* **1994**, *32*, 735–741. [[CrossRef](#)]
89. Jacimovski, S.; Bukurov, M.; Setrajcic, J.; Al, E. Phonon thermal conductivity of graphene. *Superlattices Microstruct.* **2015**, *88*, 330–337. [[CrossRef](#)]
90. Progelhof, R.C.; Throne, J.L.; Ruetsch, R.R. Methods for predicting the thermal conductivity of composite systems: A review. *Polym. Eng. Sci.* **1976**, *16*, 615–625. [[CrossRef](#)]
91. Davis, L.C.; Artz, B.E. Thermal conductivity of metal-matrix composites Thermal conductivity of metal-matrix composites. *J. Appl. Phys.* **1995**, *77*, 849–855. [[CrossRef](#)]
92. Wejrzanowski, T.; Grybczuk, M.; Chmielewski, M.; Pietrzak, K.; Kurzydowski, K.J.; Strojny-nedza, A. Thermal conductivity of metal-graphene composites. *Mater. Des.* **2016**, *99*, 163–173. [[CrossRef](#)]
93. Sajjadi, S.A.; Ezatpour, H.R.; Parizi, M.T. Comparison of microstructure and mechanical properties of A356 aluminum alloy / Al<sub>2</sub>O<sub>3</sub> composites fabricated by stir and compo-casting processes. *Mater. Des.* **2012**, *34*, 106–111. [[CrossRef](#)]
94. Habibnejad-Korayem, M.; Mahmudi, R.; Poole, W.J. Enhanced properties of Mg-based nano-composites reinforced with Al<sub>2</sub>O<sub>3</sub> nano-particles. *Mater. Sci. Eng. A* **2009**, *519*, 198–203. [[CrossRef](#)]
95. Erman, A.; Groza, J.; Li, X.; Choi, H.; Cao, G. Nanoparticle effects in cast Mg-1 wt % SiC nano-composites. *Mater. Sci. Eng. A* **2012**, *558*, 39–43. [[CrossRef](#)]
96. Pérez-Bustamante, R.; Gómez-Esparza, C.D.; Estrada-Guel, I.; Miki-Yoshida, M.; Licea-Jiménez, L.; Pérez-García, S.A.; Martínez-Sánchez, R. Microstructural and mechanical characterization of Al–MWCNT composites produced by mechanical milling. *Mater. Sci. Eng. A* **2009**, *502*, 159–163. [[CrossRef](#)]
97. Zhang, Z.; Chen, D.L. Consideration of Orowan strengthening effect in particulate-reinforced metal matrix nanocomposites: A model for predicting their yield strength. *Scr. Mater.* **2006**, *54*, 1321–1326. [[CrossRef](#)]
98. Zhang, Z.; Chen, D.L. Contribution of Orowan strengthening effect in particulate-reinforced metal matrix nanocomposites. *Mater. Sci. Eng. A* **2008**, *483–484*, 148–152. [[CrossRef](#)]
99. Humphreys, F.J.; Hatherly, M. *Recrystallization and Related Annealing Phenomena*, 2nd ed.; Elsevier: Amsterdam, The Netherlands, 2004.
100. Saboori, A. Metal Matrix Nanocomposites—Potentials, Challenges and Feasible Solutions. Ph.D. Thesis, Politecnico di Torino, Torino, Italy, 2017.
101. Arsenault, R.J.; Shi, N. Dislocation generation due to differences between the coefficients of thermal expansion. *Mater. Sci. Eng.* **1986**, *81*, 175–187. [[CrossRef](#)]
102. Sanaty-Zadeh, A. Comparison between current models for the strength of particulate-reinforced metal matrix nanocomposites with emphasis on consideration of Hall–Petch effect. *Mater. Sci. Eng. A* **2012**, *531*, 112–118. [[CrossRef](#)]
103. Landry, K.; Kalogeropoulou, S.; Eustathopoulos, N. Wettability of carbon by aluminum and aluminum alloys. *Mater. Sci. Eng. A* **1998**, *254*, 99–111. [[CrossRef](#)]
104. Rodriguez-Reyes, M.; Pech-Canul, M.I.; Rendon-Angeles, J.C.; Lopez-Cuevas, J. Limiting the development of Al<sub>4</sub>C<sub>3</sub> to prevent degradation of Al/SiC p composites processed by pressureless infiltration. *Compos. Sci. Technol.* **2006**, *66*, 1056–1062. [[CrossRef](#)]

105. Maqbool, A.; Hussain, M.A.; Khalid, F.A.; Bakhsh, N.; Hussain, A.; Ho, M. Mechanical characterization of copper coated carbon nanotubes reinforced aluminum matrix composites. *Mater. Charact.* **2013**, *86*, 39–48. [[CrossRef](#)]
106. Singh, B.B.; Balasubramanian, M. Processing and properties of copper-coated carbon fibre reinforced aluminum alloy composites. *J. Mater. Process. Technol.* **2009**, *209*, 2104–2110. [[CrossRef](#)]
107. Wang, C.; Chen, G.; Wang, X.U.; Zhang, Y. Effect of Mg Content on the thermodynamics of interface reaction in C<sub>f</sub>/Al composite. *Met. Mater. Trans. A* **2012**, *43*, 2514–2519. [[CrossRef](#)]
108. Wu, J.; Zhang, H.; Zhang, Y.; Li, J.; Wang, X. Effect of copper content on the thermal conductivity and thermal expansion of Al–Cu/diamond composites. *Mater. Des.* **2012**, *39*, 87–92. [[CrossRef](#)]
109. Fan, T.; Yang, G.; Zhang, D. Prediction of chemical stability in SiC p/Al composites with alloying element addition using Wilson equation and an extended Miedema model. *Mater. Sci. Eng. A* **2005**, *394*, 327–338. [[CrossRef](#)]
110. Liu, J.; Khan, U.; Coleman, J.; Fernandez, B.; Rodriguez, P.; Naher, S.; Brabazon, D. Graphene oxide and graphene nanosheet reinforced aluminum matrix composites: Powder synthesis and prepared composite characteristics. *Mater. Des.* **2016**, *94*, 87–94. [[CrossRef](#)]
111. Bhadauria, A.; Singh, L.K.; Laha, T. Effect of Physio-chemically functionalized graphene nanoplatelets reinforcement on tensile properties of aluminum nanocomposite synthesized via spark plasma sintering. *J. Alloys Compd.* **2018**, *748*, 783–793. [[CrossRef](#)]
112. Garbiec, D.; Jurczyk, M.; Levintant-zayonts, N.; Mo, T. Properties of Al–Al<sub>2</sub>O<sub>3</sub> composites synthesized by spark plasma sintering method. *Arch. Civ. Mech. Eng.* **2015**, *15*, 933–939. [[CrossRef](#)]
113. Arsalan, G.; Kara, F.; Turan, S. Quantitative X-ray diffraction analysis of reactive infiltrated boron carbide–aluminium composites. *J. Eur. Ceram. Soc.* **2003**, *23*, 1243–1255. [[CrossRef](#)]
114. Ghasali, E.; Alizadeh, M.; Ebadzadeh, T. Mechanical and microstructure comparison between microwave and spark plasma sintering of Al-B<sub>4</sub>C composite. *J. Alloys Compd.* **2016**, *655*, 93–98. [[CrossRef](#)]
115. Abdizadeh, H.; Ebrahimifard, R.; Baghchesara, M.A. Composites: Part B Investigation of microstructure and mechanical properties of nano MgO reinforced Al composites manufactured by stir casting and powder metallurgy methods: A comparative study. *Compos. Part B* **2014**, *56*, 217–221. [[CrossRef](#)]
116. Chawla, N.; Deng, X.; Schnell, D.R.M. Thermal expansion anisotropy in extruded SiC particle reinforced 2080 aluminum alloy matrix composites. *Mater. Sci. Eng. A* **2006**, *426*, 314–322. [[CrossRef](#)]
117. Boostani, A.F.; Tahamtan, S.; Jiang, Z.Y.; Wei, D.; Yazdani, S.; Khosroshahi, R.A.; Mousavian, R.T.; Xu, J.; Zhang, X.; Gong, D. Enhanced tensile properties of aluminium matrix composites reinforced with graphene encapsulated SiC nanoparticles. *Compos. Part A* **2015**, *68*, 155–163. [[CrossRef](#)]
118. Zhang, Q.; Ma, X.; Wu, G. Interfacial microstructure of SiCp/Al composite produced by the pressureless infiltration technique. *Ceram. Int.* **2013**, *39*, 4893–4897. [[CrossRef](#)]
119. Bartolucci, S.F.; Paras, J.; Rafiee, M.A.; Rafiee, J.; Lee, S.; Kapoor, D.; Koratkar, N. Graphene–aluminum nanocomposites. *Mater. Sci. Eng. A* **2011**, *528*, 7933–7937. [[CrossRef](#)]
120. Li, J.L.; Xiong, Y.C.; Wang, X.D.; Yan, S.J.; Yang, C.; He, W.W.; Chen, J.Z.; Wang, S.Q.; Zhang, X.Y.; Dai, S.L. Microstructure and tensile properties of bulk nanostructured aluminum/graphene composites prepared via cryomilling. *Mater. Sci. Eng. A* **2015**, *626*, 400–405. [[CrossRef](#)]
121. Hu, Z.; Chen, F.; Xu, J.; Nian, Q.; Lin, D.; Chen, C.; Zhu, X.; Chen, Y.; Zhang, M. 3D printing graphene-aluminum nanocomposites. *J. Alloys Compd.* **2018**, *746*, 269–276. [[CrossRef](#)]
122. Zhao, R.; Xu, R.; Fan, G.; Chen, K.; Tan, Z.; Xiong, D.; Li, Z.; Dmitrievich, S.; Zhang, D. Reinforcement with in-situ synthesized carbon nano-onions in aluminum composites fabricated by flake powder metallurgy. *J. Alloys Compd.* **2015**, *650*, 217–223. [[CrossRef](#)]
123. Cao, L.; Li, Z.; Kim, Y.; Fan, G.; Jiang, L.; Zhang, D.; Moon, W. The growth of carbon nanotubes in aluminum powders by the catalytic pyrolysis of polyethylene glycol. *Carbon N. Y.* **2011**, *50*, 1057–1062. [[CrossRef](#)]
124. Shin, S.E.; Choi, H.J.; Shin, J.H.; Bae, D.H. Strengthening behavior of few-layered graphene/aluminum composites. *Carbon N. Y.* **2014**, *82*, 143–151. [[CrossRef](#)]
125. Yan, S.J.; Dai, S.L.; Zhang, X.Y.; Yang, C.; Hong, Q.H.; Chen, J.Z.; Lin, Z.M. Investigating aluminum alloy reinforced by graphene nano flakes. *Mater. Sci. Eng. A* **2014**, *612*, 440–444. [[CrossRef](#)]
126. Rashad, M.; Pan, F.; Yu, Z.; Asif, M. Investigation on microstructural, mechanical and electrochemical properties of aluminum composites reinforced with graphene nanoplatelets. *Prog. Nat. Sci. Mater. Int.* **2015**, *25*, 460–470. [[CrossRef](#)]

127. Reddy, K.S.; Sreedhar, D.; Kumar, K.D.; Kumar, G.P. Role of reduced graphene oxide on mechanical-thermal properties of aluminum metal matrix nano composites. *Mater. Today Proc.* **2015**, *2*, 1270–1275. [[CrossRef](#)]
128. Bastwros, M.; Kim, G.; Zhu, C.; Zhang, K.; Wang, S.; Tang, X.; Wang, X. Effect of ball milling on graphene reinforced Al6061 composite fabricated by semi-solid sintering. *Compos. Part B* **2014**, *60*, 111–118. [[CrossRef](#)]
129. Saboori, A.; Novara, C.; Pavese, M.; Badini, C.; Giorgis, F.; Fino, P. An investigation on the sinterability and the compaction behavior of aluminum/graphene nanoplatelets (GNPs) prepared by powder metallurgy. *J. Mater. Eng. Perform.* **2017**, *26*, 993–999. [[CrossRef](#)]
130. Saboori, A.; Pietroluongo, M.; Pavese, M.; Badini, C.; Fino, P. Influence of graphene nanoplatelets (GNPs) on compressibility and sinterability of Al matrix nanocomposites prepared by powder metallurgy. In Proceedings of the World PM 2016 Congress and Exhibition, Hamburg, Germany, 9–13 October 2016.
131. Saboori, A.; Pavese, M.; Badini, C.; Fino, P. Microstructure and thermal conductivity of Al-Graphene composites fabricated by powder metallurgy and hot rolling techniques. *Acta Met. Sin.* **2017**, *30*, 675–687. [[CrossRef](#)]
132. Saboori, A.; Casati, R.; Zanatta, A.; Pavese, M.; Badini, C.; Vedani, M. Effect of graphene nanoplatelets on microstructure and mechanical properties of AlSi<sub>10</sub>Mg nanocomposites produced by hot extrusion. *Powder Metall. Met. Ceram.* **2018**, *56*, 647–655. [[CrossRef](#)]
133. Chen, B.; Bi, Q.; Yang, J.; Xia, Y.; Hao, J. Tribology international tribological properties of solid lubricants (graphite, h-BN) for Cu-based P/M friction composites. *Tribol. Int.* **2008**, *41*, 1145–1152. [[CrossRef](#)]
134. Hanada, K.; Matsuzaki, K.; Sano, T. Thermal properties of diamond particle-dispersed Cu composites. *J. Mater. Process. Technol.* **2004**, *153–154*, 514–518. [[CrossRef](#)]
135. Davis, J.R. Powder metallurgy: Copper and copper alloys. In *ASM Specialty Handbook*; ASM International: Materials Park, OH, USA, 2001; ISBN 0-87170-726-8.
136. Nadkarani, A. Dispersion Strengthened Metal Composites. U.S. Patent 4,752,334, 21 June 1988.
137. Caron, R.N. *Copper Alloys: Properties and Applications*, 2nd ed.; ASM International: Materials Park, OH, USA, 2001.
138. Kundig, K.J.A.; Cowie, J.G. *Mechanical Engineers' Handbook: Materials and Mechanical Design*, 3rd ed.; Kutz, M., Ed.; John Wiley & Sons, Inc.: Hoboken, NJ, USA, 2006; ISBN 9780471449904.
139. Zhao, S.; Zheng, Z.; Huang, Z.; Dong, S.; Luo, P.; Zhang, Z.; Wang, Y. Cu matrix composites reinforced with aligned carbon nanotubes: Mechanical, electrical and thermal properties. *Mater. Sci. Eng. A* **2016**, *675*, 82–91. [[CrossRef](#)]
140. Yao, G.C.; Mei, Q.S.; Li, J.Y.; Li, C.L.; Ma, Y.; Chen, F.; Liu, M. Cu/C composites with a good combination of hardness and electrical conductivity fabricated from Cu and graphite by accumulative roll-bonding. *Mater. Des.* **2016**, *110*, 124–129. [[CrossRef](#)]
141. Arnaud, C.; Lecouturier, F.; Mesguich, D.; Ferreira, N.; Chevallerier, G.; Estournes, C.; Weibel, A.; Laurent, C. High strength and high conductivity double-walled carbon nanotube—Copper composite wires. *Carbon N. Y.* **2016**, *96*, 212–215. [[CrossRef](#)]
142. Saboori, A.; Pavese, M.; Badini, C.; Fino, P. A Novel Cu-GNPs Nanocomposite with improved thermal and mechanical properties. *Acta Met. Sin.* **2018**, *31*, 148–152. [[CrossRef](#)]
143. Saboori, A.; Moheimani, S.K.; Pavese, M.; Badini, C.; Fino, P. New Nanocomposite materials with improved mechanical strength and tailored coefficient of thermal expansion for electro-packaging applications. *Metals* **2017**, *7*, 536. [[CrossRef](#)]
144. Chu, K.; Wang, F.; Wang, X.; Huang, D. Anisotropic mechanical properties of graphene/copper composites with aligned graphene. *Mater. Sci. Eng. A* **2018**, *713*, 269–277. [[CrossRef](#)]
145. Varol, T.; Canakci, A. Microstructure, electrical conductivity and hardness of multilayer graphene/copper nanocomposites synthesized by flake powder metallurgy. *Met. Mater. Int.* **2015**, *21*, 704–712. [[CrossRef](#)]
146. Varol, T.; Canakci, A. Effect of the CNT content on microstructure, physical and mechanical properties of Cu-based electrical contact materials produced by flake powder metallurgy. *Arab. J. Sci. Eng.* **2015**, *40*, 2711–2720. [[CrossRef](#)]
147. Mai, Y.J.; Chen, F.X.; Lian, W.Q.; Zhang, L.Y.; Liu, C.S.; Jie, X.H. Preparation and tribological behavior of copper matrix composites reinforced with nickel nanoparticles anchored graphene nanosheets. *J. Alloys Compd.* **2018**, *756*, 1–7. [[CrossRef](#)]
148. Moustafa, S.F.; El-Badry, S.A.; Sanad, A.M.; Kieback, B. Friction and wear of copper-graphite composites made with Cu-coated and uncoated graphite powders. *Wear* **2002**, *253*, 699–710. [[CrossRef](#)]

149. Moustafa, S.F.; El-Badry, S.A.; Sanad, A.M. Effect of graphite with and without copper coating on consolidation behaviour and sintering of copper-graphite composite. *Powder Met.* **1997**, *40*, 201–206. [[CrossRef](#)]
150. Dey, A.; Pandey, K.M. Magnesium metal matrix composites—A review. *Rev. Adv. Mater. Sci.* **2015**, *42*, 58–67.
151. Ye, H.; Liu, X.Y. Review of recent studies in magnesium. *J. Mater. Sci.* **2004**, *39*, 6153–6171. [[CrossRef](#)]
152. Xiuqing, Z.; Haowei, W.; Lihua, L.; Xinying, T.; Naiheng, M. The mechanical properties of magnesium matrix composites reinforced with (TiB<sub>2</sub> + TiC) ceramic particulates. *Mater. Lett.* **2005**, *59*, 2105–2109. [[CrossRef](#)]
153. Hou, L.G.; Wu, R.Z.; Wang, X.D.; Zhang, J.H.; Zhang, M.L.; Dong, A.P.; Sun, B.D. Microstructure, mechanical properties and thermal conductivity of the short carbon fiber reinforced magnesium matrix composites. *J. Alloys Compd.* **2016**, *695*, 2820–2826. [[CrossRef](#)]
154. Suresh, M.; Srinivasan, A.; Pillai, U.T.S.; Pai, B.C. The effect of charcoal addition on the grain refinement and ageing response of magnesium alloy AZ91. *Mater. Sci. Eng. A* **2011**, *528*, 8573–8578. [[CrossRef](#)]
155. Rashad, M.; Pan, F.; Tang, A.; Asif, M.; Hussain, S.; Gou, J.; Mao, J. Improved strength and ductility of magnesium with addition of aluminum and graphene nanoplatelets (Al + GNPs) using semi powder metallurgy method. *J. Ind. Eng. Chem.* **2015**, *23*, 243–250. [[CrossRef](#)]
156. Rafiee, M.A.; Rafiee, J.; Wang, Z.; Song, H.; Yu, Z.-Z.; Koratkar, N. Enhanced mechanical properties of nanocomposites at low graphene content. *ACS Nano* **2009**, *3*, 3884–3890. [[CrossRef](#)] [[PubMed](#)]
157. Shi, D.L.; Feng, X.Q.; Huang, Y.Y.; Hwang, K.C. Critical Evaluation of the Stiffening Effect of Carbon Nanotubes in Composites. In *Advances in Fracture and Failure Prevention; Key Engineering Materials*; Trans Tech Publications: Zürich, Switzerland, 2004; Volume 261, pp. 1487–1492.
158. Habibi, M.K.; Paramsothy, M.; Hamouda, A.M.S.; Gupta, M. Using integrated hybrid (Al + CNT) reinforcement to simultaneously enhance strength and ductility of magnesium. *Compos. Sci. Technol.* **2011**, *71*, 734–741. [[CrossRef](#)]
159. Sankaranarayanan, S.; Jayalakshmi, S.; Gupta, M. Effect of ball milling the hybrid reinforcements on the microstructure and mechanical properties of Mg–(Ti + n-Al<sub>2</sub>O<sub>3</sub>) composites. *J. Alloys Compd.* **2011**, *509*, 7229–7237. [[CrossRef](#)]
160. Tun, K.S.; Tungala, V.; Nguyen, Q.B.; Chan, J.; Kwok, R.; Kuma, J.V.M.; Gupta, M. Enhancing tensile and compressive strengths of magnesium using nanosize (Al<sub>2</sub>O<sub>3</sub> + Cu) hybrid reinforcements. *J. Compos. Mater.* **2012**, *46*, 1879–1887. [[CrossRef](#)]
161. Sankaranarayanan, S.; Jayalakshmi, S.; Gupta, M. Effect of individual and combined addition of micro/nano-sized metallic elements on the microstructure and mechanical properties of pure Mg. *Mater. Des.* **2012**, *37*, 274–284. [[CrossRef](#)]
162. Gupta, M.; Lai, M.O.; Saravanaranganathan, D. Synthesis, microstructure and properties characterization of disintegrated melt deposited Mg/SiC composites. *J. Mater. Sci.* **2000**, *35*, 2155–2165. [[CrossRef](#)]
163. Chua, B.W.; Lu, L.; Lai, M.O. Influence of SiC particles on mechanical properties of Mg based composite. *Compos. Struct.* **1999**, *47*, 595–601. [[CrossRef](#)]

